 © 2016 Russian Academy of Sciences and Turpion Ltd

DOI 10.1070/RCR4489

Phase equilibria in fullerene-containing systems as a basis for development of manufacture and application processes for nanocarbon materials

K N Semenov,[a] N A Charykov,[b] V N Postnov,[a] V V Sharoyko,[a] I V Murin [a]

[a] *Saint Petersburg State University*
Universitetskaya nab. 7/9, 199034 St Petersburg, Russian Federation
[b] *Saint Petersburg State Institute of Technology (Technical University)*
Moskovskii prosp. 26, 190013 St Petersburg, Russian Federation

This review is the first attempt to integrate the available data on all types of phase equilibria (solubility, extraction and sorption) in systems containing light fullerenes (C_{60} and C_{70}). In the case of solubility diagrams, the following types of phase equilibria are considered: individual fullerene (C_{60} or C_{70}) – solvent under polythermal and polybaric conditions; C_{60} – C_{70} – solvent, individual fullerene – solvent(1) – solvent(2), as well as multicomponent systems comprising a single fullerene or an industrial mixture of fullerenes and vegetable oils, animal fats or essential oils under polythermal conditions. All published experimental data on the extraction equilibria in C_{60} – C_{70} – liquid phase(1) – liquid phase(2) systems are described systematically and the sorption characteristics of various materials towards light fullerenes are estimated. The possibility of application of these experimental data for development of pre-chromatographic and chromatographic methods for separation of fullerene mixtures and application of fullerenes as nanomodifiers are described.
The bibliography includes 87 references.

Contents

I. Introduction 38
II. Solubility diagrams of the binary, ternary and multicomponent systems containing light fullerenes 39
III. Extraction equilibria in systems containing light fullerenes 50
IV. Sorption equilibria in systems containing light fullerenes 56

I. Introduction

The physical chemistry of nanostructures, in particular, carbon nanoclusters, fullerenes and their derivatives, is among the most vigorously developing areas of modern chemistry. This is due to the fact that fullerenes (the only soluble molecular form of carbon) are unique objects as regards the electronic structure and physical and chemical properties. Hence, study of the phase equilibria in fullerene-containing systems is of primary significance for the development of crystallization- and extraction-based processes for recovery of fullerenes from fullerene carbon black or

K N Semenov Candidate of Chemical Sciences, Associate Professor of the Department of Solid State Chemistry at the Institute of Chemistry, SPbSU.
E-mail: semenov1986@yandex.ru
Current research interests: chemistry of carbon nanostructures, thermodynamics of heterogeneous systems.
N A Charykov Doctor of Chemical Sciences, Professor of the Department of Physical Chemistry at the SPbSIT (TU).
Telephone: +7(812)347 – 6597, e-mail: ncharykov@yandex.ru
Current research interests: chemistry and physics of carbon nanostructures, thermodynamics of heterogeneous systems, thermodynamics of solutions.
V N Postnov Candidate of Chemical Sciences, Associate Professor of the Department of Solid State Chemistry at the Institute of Chemistry, SPbSU.
Telephone: +7(812)428 – 4136, e-mail: postnovvn@rambler.ru
Current research interests: surface chemistry, heterogeneous catalysis, adsorption.
V V Sharoyko Doctor of Biological Sciences, Leading Researcher of the Laboratory of Biomedical Chemistry at the Institute of Chemistry, SPbSU.
E-mail: v.sharoyko@spbu.ru
Current research interests: molecular recognition, biocatalysis, molecular signalling, molecular biotechnology.
I V Murin Doctor of Chemical Sciences, Professor, Head of the Department of Solid State Chemistry at the Institute of Chemistry, SPbSU.
Telephone: +7(812)428 – 6859, e-mail: igormurin@mail.ru
Current research interests: solid state ionics, nanocarbon materials, nanotechnologies.

Received 30 July 2014
Uspekhi Khimii **85** (1) 38 – 59 (2016); translated by Z P Svitanko

fullerene mixtures, for the development of chromatographic and pre-chromatographic processes of fullerene separation, for investigation of homogeneous chemical reactions involving fullerenes and for optimization of fullerene application as nanomodifiers for polymers. The topicality of this research is evidenced by the huge array of published experimental data on isothermal solubility of light fullerenes. Indeed, the solubility of C_{60} in more than 150 solvents and the solubility of C_{70} in 40 solvents have been studied, organic and inorganic compounds of various classes being used as solvents (aromatic hydrocarbons, alkanes, cycloalkanes, haloalkanes, alcohols, *etc.*). In the last decade, two reviews were published devoted to the solubility diagrams of systems containing light fullerenes and solutions of fullerenes and their derivatives in various solvents.[1,2] The fundamental distinction of this review is systematic account of all the available data on the phase equilibria in light fullerene-containing systems — experimental data on the phase equilibria arising during dissolution, extraction and sorption.

II. Solubility diagrams of the binary, ternary and multicomponent systems containing light fullerenes

Analysis of literature data on the solubility of individual light fullerenes C_{60} and C_{70} at room temperature (experimental data on the isothermal solubility of individual light fullerenes are summarized in Tables 1, 2 of the Electronic Supplement)† reveals a number of regular patterns. The solubility of individual light fullerenes (C_{60} or C_{70}) has the same order of magnitude but can differ several-fold; this difference can provide grounds for one of the most efficient methods for the separation of industrial mixtures of fullerenes. Fullerenes are almost insoluble in polar solvents and poorly soluble in acyclic saturated hydrocarbons; the solubility in the latter increases with increasing number of carbon atoms; this, in turn, attests to the insignificant role of the solvation mechanism of dissolution. The highest solubility of fullerenes is observed for such solvents for which the specific enthalpy of dissolution divided by the volume of the solvent molecule is close to this value for fullerene.[2–5] Such solvents are, for example, aromatic hydrocarbons and their derivatives.[3–5] Experimental data on the polythermal solubility of fullerenes C_{60} and C_{70} and an industrial fullerene mixture [C_{60} (60% – 65%) + C_{70} (33% – 39%) + C_{76-90} (1% – 2%)] in various organic and inorganic solvents are summarized in Tables 3 and 4 of the electronic supplement. It is noteworthy that the study of solubility diagrams of ternary systems is of obvious practical interest. This is due to the fact that it is possible to separate fullerene mixture components on the basis of different solubility of fullerenes (first of all, the major components of the mixture — C_{60} and C_{70}).[3,6–9]

II.1. Effect of temperature on the solubility of fullerenes. Thermodynamic description of the phase equilibria of the solubility in systems containing light fullerenes

The dissolution of fullerenes consists of several stages accompanied by particular energy effects: the endothermic destruction of the fullerite crystal lattice and cleavage of bonds between solvent molecules and the exothermic solvation (physical or chemical), which counterbalances this energy expenditure in those cases where the molecular fields of the solvent and the solute are similar (Semenchenko's rule) and there is also interaction between the solute and the solvent.[10] Unlike most non-polar organic solvents, the enthalpy of dissolution of C_{60} is negative (the dissolution is exothermic). Hence, according to vant Hoff's equation reflecting the temperature dependence of the solubility, the solubility should decrease with increasing temperature, which is untypical of non-electrolytes and which is actually observed after the invariant point of maximum solubility (Fig. 1) where a first-order phase transition takes place upon the loss of a solvation shell (point ○).[1,3,4,18] Dependences of this sort were elucidated for the first time by Ruoff *et al.*[3] for the C_{60} – hexane, C_{60} – toluene and C_{60} – carbon disulfide systems. This type of temperature dependence of the solubility is rather frequent for binary water–salt systems (for example, $NaF-H_2O$, CaF_2-H_2O, $NH_4HF_2-H_2O$, $ZrOCl_2-H_2O$, $MgSO_3-H_2O$, $CuSO_4-H_2O$ and so on)[19] (Fig. 2). Meanwhile, the solubility polytherm of C_{70} in 1,2-dimethylbenzene has a sigmoid shape, which reflects the solvate-free nature of dissolution (see Fig. 1). Gardette *et al.*[21] constructed the 'approximate' phase diagram for the C_{60} – sulfur binary system (Fig. 3) in the case where dissolution proceeds *via* the formation of the fullerene solvate. Phase diagrams of this type were also obtained for C_{60} – bromobenzene and C_{60} – 1,2-dimethylbenzene systems.[21–25] If desolvation occurs in several stages [for example, according to Eqns (1) and (2), B is solvent]

$$C_{60}\cdot n\,B(s) = C_{60}\cdot m\,B(s) + (n-m)\,B(liq) \quad (1)$$

$$C_{60}\cdot m\,B(s) = C_{60}(s) + m\,B(liq) \quad (2)$$

the solubility diagram has two peritectic points (points *O* and *O′* in Fig. 4). This type of phase diagrams was detected for binary systems C_{60} – 1,3-$X_2C_6H_4$ (X = Me, Cl, Br).[24] By

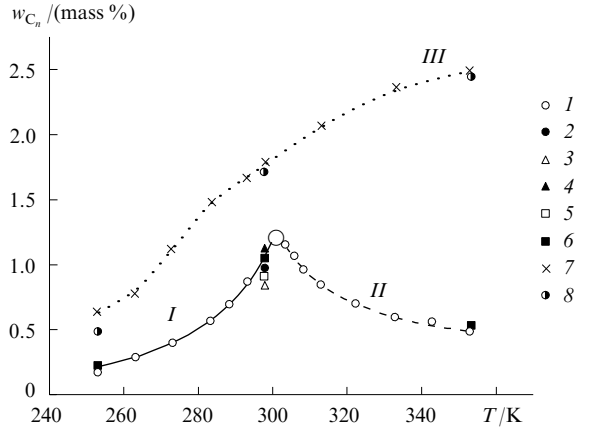


Figure 1. Temperature dependences of the solubility of fullerenes C_{60} (*I* and *II*) and C_{70} (*III*) in 1,2-dimethylbenzene.
Line *I* corresponds to the crystallization of the solvate $C_{60}\,2(1,2\text{-}Me_2C_6H_4)$, line *II* is the crystallization of non-solvated C_{60}. Point ○ is the dissociation point of the bisolvate $C_{60}\,2(1,2\text{-}Me_2C_6H_4)$ according to the reaction $C_{60}\,2(1,2\text{-}Me_2C_6H_4)(s) \rightarrow C_{60}(s) + 2(1,2\text{-}Me_2C_6H_4)(liq)$; (*1*) see Ref. 11, (*2*) see Ref. 12, (*3*) see Ref. 13, (*4*) see Ref. 14, (*5*) see Ref. 15, (*6*) see Ref. 16, (*7*) see Ref. 11, (*8*) see Ref. 17.

† For Electronic Supplement, see www.iopscience.iop.org/0036-021X.

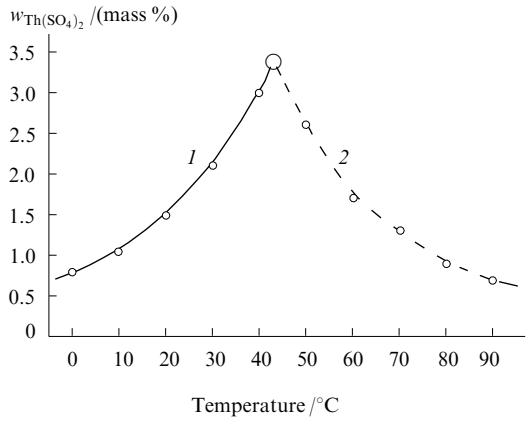


Figure 2. Temperature dependence of the water solubility of thorium sulfate.[20]
Line *1* corresponds to the crystallization of crystalline hydrate $Th(SO_4)_2 \cdot 9\,H_2O$, line *2* shows the crystallization of $Th(SO_4)_2 \cdot 5\,H_2O$. Point ○ is the dissociation point of the crystalline hydrate $Th(SO_4)_2 \cdot 9\,H_2O$ according to the reaction $Th(SO_4)_2 \cdot 9\,H_2O(s) \rightarrow Th(SO_4)_2 \cdot 5\,H_2O(s) + 4\,H_2O(liq)$.

now, the formation of solid crystalline solvates has been established for more than 50 binary systems formed by a fullerene (C_{60} or C_{70}) and a solvent (data on the composition of crystalline solvates of light fullerenes are summarized in Table 5 of the electronic supplement).

We will briefly consider the theories that account for the non-monotonic temperature dependences of solubility. For example, Bezmel'nitsyn *et al.*[5,26] constructed a statistical model that interpreted the non-monotonic temperature dependence of the solubility as being due to a first order phase transition in crystalline C_{60}, which occurs at 260 K and results in orientational disorder of molecules and rearrangement of the crystal structure. The authors suggested the formation of fullerene clusters (aggregates containing 5–40 C_{60} molecules) in the polytherm segment characterized by an increase in the solubility up to the maximum solubility point (260 K). In turn, the branch describing the decrease in the solubility corresponds to

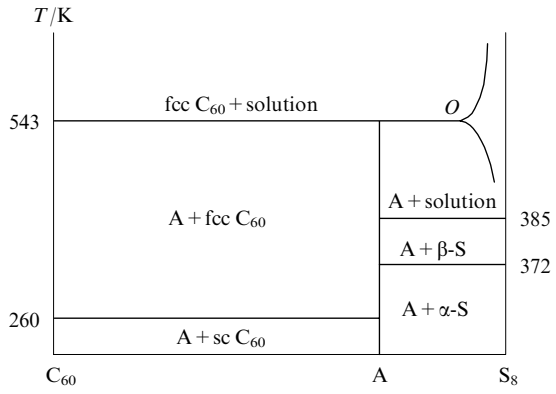


Figure 3. Phase diagram of the $C_{60}-S$ system.[21]
Point *O* is the invariant point of maximum solubility in which incongruent melting of the solvate takes place; fcc C_{60} is the face centred cubic lattice of C_{60}, sc C_{60} is simple cubic lattice of C_{60}, A is the monoclinic phase of $C_{60} \cdot 2\,S_8$.

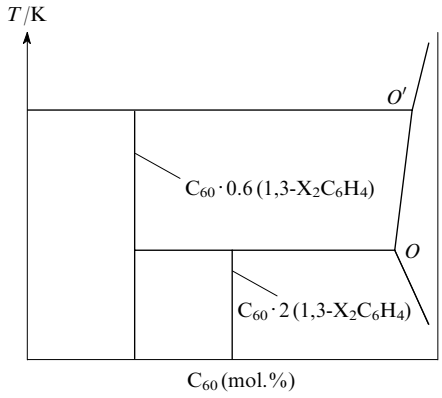


Figure 4. Phase diagram of the $C_{60}-1,3\text{-}X_2C_6H_4$ system (X = Me, Cl, Br).[24]

thermal destruction of fullerene aggregates.[5,26] However, the proposed theory cannot explain the difference between the temperatures of maximum solubility in the series of C_{60}–solvent binary systems including hexane, toluene, carbon disulfide, *o*-xylene, as the theory assumes that the maximum solubility temperature corresponds to the phase transition (260 K) in crystalline C_{60}.

One more thermodynamic model describing the non-monotonic pattern of temperature dependences of solubility was developed by Korobov and co-workers.[22,23,27] These authors proposed equations describing the solubility curves before and after the invariant point of maximum solubility (see Fig. 2). By setting the condition of simultaneous chemical and phase equilibria in both branches (low-temperature and high-temperature) of the solubility polytherm, the authors derived Eqn (3) for the low-temperature branch and Eqn (4) (Vant Hoff's equation) for the high-temperature branch.[18,20,28]

$$\left(\frac{\mathrm{d}x_{C_{60}}^{(l)}}{\mathrm{d}T}\right)_p = \frac{\Delta h_{C_{60}}^{solv} - [\Delta h(kC_{60}lB)/k]}{RT^2} \quad (3)$$

$$\left(\frac{\mathrm{d}\ln x_{C_{60}}^{(l)}}{\mathrm{d}T}\right)_p = \frac{\Delta h_{C_{60}}^{solv}}{RT^2} \quad (4)$$

Here $\Delta h_{C_{60}}^{solv}$ is the partial molar enthalpy of dissolution of C_{60} to give a saturated solution with the mole fraction of the solute $x_{C_{60}}^{(l)}$; $\Delta h(kC_{60} \cdot lB)$ is the heat of formation of the solvate from pure fullerene and solvent; k, l are the stoichiometric coefficients for the formation of fullerene solvate by the reaction

$$kC_{60}(liq) + lB(liq) = kC_{60}lB(s)$$

T is the absolute temperature; R is the universal gas constant.

It should be emphasized that Eqns (3) and (4) were obtained with the assumption that solutions of fullerenes are pseudo-ideal, which implies that the activity coefficient of fullerene in a saturated solution is constant and independent (or negligibly dependent) of temperature and composition over the whole concentration range. The deviations from ideality can be either positive (in the case of association of fullerene molecules) or negative (for example, for

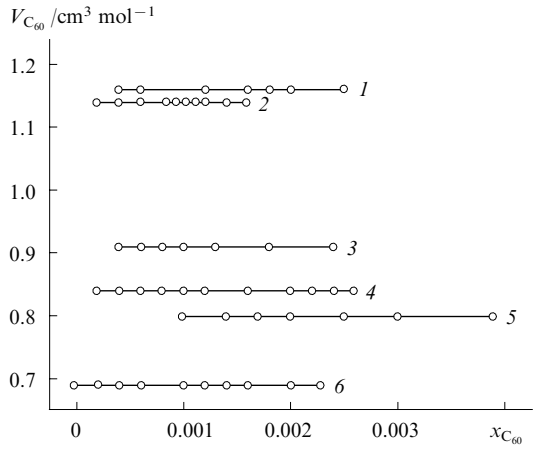


Figure 5. Partial molar volume of C_{60} [$V(C_{60})$] *vs.* mole fraction of C_{60} in the solution.[29]
(*1*) Toluene, (*2*) benzene, (*3*) chlorobenzene, (*4*) 1-chloronaphthalene, (*5*) CS_2, (*6*) 1,2,4-trichlorobenzene.

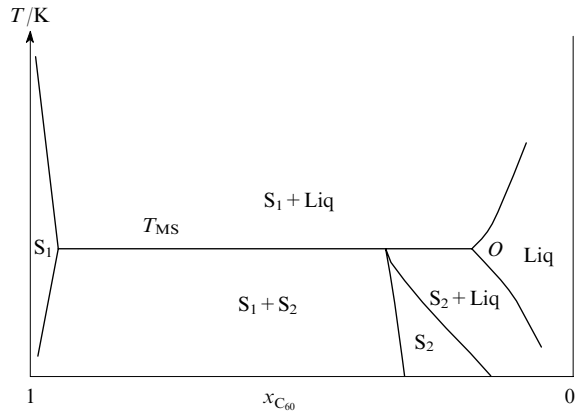


Figure 7. Phase diagram of the binary system C_{60} – solvent in the case of formation of solid solutions;[27]
S_1, S_2 are solid solutions; $S_1 + S_2$ is the monovariant region corresponding to the break of continuity; *O* is the peritectic point corresponding to the maximum solubility; on the right of this point is the bivariant region of existence of the solution; T_{MS} is the maximum solubility temperature.

solvation of fullerenes). Consider some pieces of evidence for the invariability of the activity coefficients of fullerenes in solutions. Ruelle *et al.*[29] ascertained the absence of a concentration dependence of the partial molar volume of C_{60} for 12 organic solvents over a broad concentration range from infinitely dilute to saturated solutions (Fig. 5).

The absence of functional dependence of the partial molar volume of C_{60} on concentration means that $\gamma(C_{60}) = 1$ (case of ideal solution) or $\gamma(C_{60}) = \text{const}$ for the whole concentration range (case of infinitely dilute solution; occurs for solutions of C_{60}).[30] The linearity of the branches of solubility polytherms in the $\ln x_{C_{60}} - 1/T$ coordinates (Fig. 6) also supports the invariability of the activity coefficient of fullerene in a saturated solution and the lack of its dependence on temperature or composition over the whole concentration range.[32] Assuming that fullerene solutions are pseudo-ideal, Semenov *et al.*[32] calculated the changes in the standard thermodynamic functions (Gibbs energy, entropy and enthalpy) at 298.15 K for dissociation of crystalline solvates that are formed by light fullerenes (C_{60} or C_{70}) in the binary systems C_{60} – n-alkanols, C_{60} – n-alkanoic acids, C_{70} – n-alkanoic acids.[32]

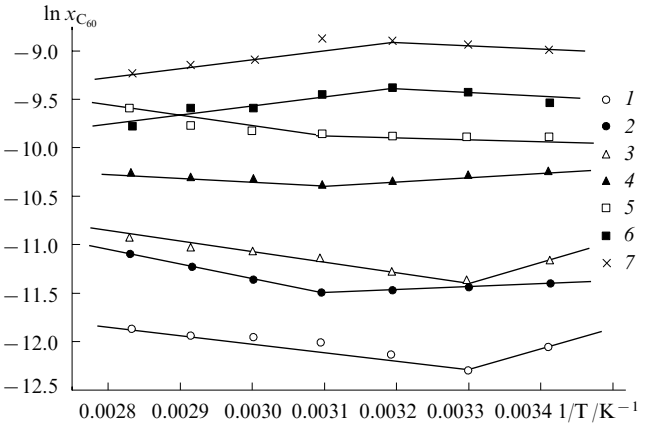


Figure 6. Solubility polytherms in the systems fullerene C_{60} – normal monohydric alcohols ($C_5 - C_{11}$).[6, 31]
(*1*) Pentanol, (*2*) hexanol, (*3*) heptanol, (*4*) octanol, (*5*) nonanol, (*6*) decanol, (*7*) undecanol.

Korobov and Smith[27] considered the formation of solid solutions of fullerenes with the solvent. It was noted that in some cases, unstable compounds are formed in the solid phase and uncontrolled loss of the solvent takes place. The formation of fullerene-based solid solutions was considered (the type of solid solutions was not discussed). For example, in the case of tetrachloromethane, different authors reported the formation of different solvates (1 : 13.7, 1 : 13, 1 : 12, 1 : 10). The authors[27] constructed a tentative phase diagram taking account of the formation of solid solutions (Fig. 7) and derived an equation for describing the temperature dependence of solubility [Eqn (5)].

$$\left(\frac{\mathrm{d}x}{\mathrm{d}T}\right)_p = \frac{x'(h^{(l)}_{C_{60}} - h^{(s)}_{C_{60}}) + (1 - x')(h^{(l)}_{B} - h^{(s)}_{B})}{T(x' - x)(\partial^2 G/\partial x^2)_{T,p}} \qquad (5)$$

Here $h^{(s)}_{C_{60}}$, $h^{(l)}_{C_{60}}$ are the partial molar enthalpies of fullerene in the solid and liquid phases; $h^{(s)}_{B}$, $h^{(l)}_{B}$ are the partial molar enthalpies of the solvent in the solid and liquid phases; x and x' are the fullerene mole fractions in the solid solution and the liquid phase, G is the Gibbs energy.

This is exemplified in Fig. 8, which shows the temperature dependences of the solubility of components of an industrial fullerene mixture in nonanol.[6] The polytherm branch before point *O* corresponds to an equilibrium of a saturated solution of fullerenes with the monosolvated substitution solid solution $(C_{60})_x(C_{70})_{1-x} \cdot n\text{-}C_9H_{19}OH$. The invariant point of solubility extremum (point *O* in Fig. 8) corresponds to incongruent melting of the solid crystalline monosolvate to give unsolvated solid solution; the high-temperature branch of the solubility polytherm indicates an equilibrium between a saturated solution and unsolvated substitution solid solution $(C_{60})_x(C_{70})_{1-x}$.

Figure 9 shows the plot for fullerene C_{60} content (%) in a saturated solution *vs.* temperature for nonyl alcohol.[6]

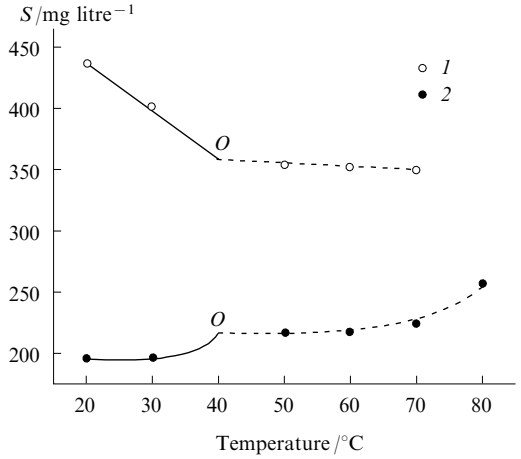


Figure 8. Polytherms of solubility of the components of an industrial fullerene mixture (C_{60} and C_{70}) in nonyl alcohol.[6]
The continuous line corresponds to the crystallization of $(C_{60})_x(C_{70})_{1-x}\cdot$n-$C_9H_{19}OH$, the dashed line corresponds to the crystallization of $(C_{60})_x(C_{70})_{1-x}$; *O* is the dissociation point of the monosolvated solid solution; (*1*) C_{60}, (*2*) C_{70}.

Analysis of the curve demonstrates that at low temperature, the liquid phase is mainly enriched with C_{60} (the enrichment is ~8% at 20 °C), while the content of C_{70} increases with increasing temperature to reach 12% at 80 °C. This difference between the fullerene contents in the initial mixture and in the solution may serve for the development of a method for a more or less complete pre-chromatographic separation of the fullerenes. Semenov *et al.*[6] investigated the issues of dissociation temperatures of fullerene solvates based on individual light fullerenes formed in individual fullerene–solvent binary systems and dissociation temperature of solvated substitution solid solutions, which are, in turn, formed in $C_{60}-C_{70}$–solvent ternary systems. Using the van der Waals equation in the metric of partial Gibbs potential (Korzhinskii potential) for desolvation of fullerene solid solutions according to the scheme

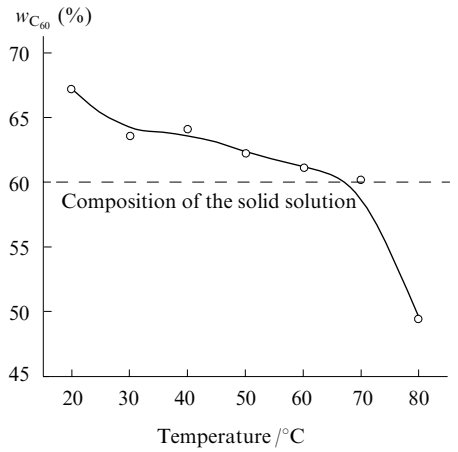


Figure 9. Temperature dependence of the content of fullerene C_{60} from the industrial fullerene mixture comprising 60% C_{60}, 39% C_{70}, 1% C_n, $n > 70$ (dashed line) in a saturated solution.[6]

$$\{(C_{60})_{Y1}(C_{70})_{1-Y1}\ q_1B\}^{(S_1)} \longrightarrow \quad (6)$$

$$\longrightarrow \{(C_{60})_{Y2}(C_{70})_{1-Y2}\ q_2B\}^{(S_2)} +$$

$$+ \{(Y_1-Y_2)C_{60}+(Y_2-Y_1)C_{70} + \Delta qB\}^{(L)}$$

where S_1 is a solid solution based on q_1-crystalline solvates of light fullerenes, S_2 is a solid solution based on q_2-crystalline solvates of light fullerenes, q_1 and q_2 are the numbers of solvent molecules in the crystalline solvate, L is a saturated liquid solution, Y_1 is the fraction of $C_{60}\cdot q_1B$ in the solid solution $\{(C_{60})_{Y1}(C_{70})_{1-Y1}\cdot q_1B\}$, Y_2 is the fraction of $C_{60}\cdot q_2B$ in the solid solution $\{(C_{60})_{Y2}(C_{70})_{1-Y2}\cdot q_2B\}$, analogues of the Gibbs–Konovalov laws were derived, the phase diagrams for coexistence of solvated and desolvated solid solutions in the solvate-free concentration space were constructed and it was proved that the dissociation temperatures of fullerene solid solutions do not coincide with the dissociation temperatures of solvated individual fullerenes.[6]

II.2. Correlation approaches to description of the solubility of fullerenes in various solvents

Among the papers devoted to the solubility of fullerenes in various solvents, a special position belongs to studies dealing with finding correlations between the solubility and molecular characteristics of the solvent. In this respect, note the pioneering study by Sivaraman *et al.*[4] considering the solubility of C_{60} in 15 polar and non-polar solvents and elucidating the correlation between the solubility and the Hildebrand solubility parameter (δ)[24,30]

$$\delta = \left(\frac{\Delta H_{vap} - RT}{V}\right)^{1/2} \quad (7)$$

where ΔH_{vap} is the vaporization enthalpy (J mol^{-1}) and V is the molar volume (mol cm^{-3}). The solubility parameter is a direct characteristics of solvent–solvent and solute–solute intermolecular interactions. As a result, the researchers cited[4] found that the fullerene solubility is maximum in those solvents for which the δ values are close to these values for the solute. According to Hildebrand's theory, the solubility parameter is defined only for the liquid state and, to define δ for fullerene, a hypothetical supercooled liquid is taken as the standard state for fullerene; furthermore, for the calculation of δ, the enthalpy of vaporization is replaced by the enthalpy of sublimation of fullerene. Sivaraman *et al.*[4] developed this approach and applied it for description of a wider range of solvents. The authors concluded that none of the solvent parameters taken alone (refractive index, dielectric constant, molar volume, *etc.*) is able to universally predict the solubility of fullerenes; however, the values of a set of parameters that can together ensure a high solubility of fullerenes were elucidated experimentally, in particular, high refractive index, dielectric constant of ~4, high molecular volume of the solvent, Hildebrand solubility parameter approaching 20 J$^{1/2}$ cm$^{-3/2}$ and a medium nucleophilicity.[4]

Herbst *et al.*[33] studied the enthalpy of dissolution of C_{60} in five solvents (benzene, toluene, bromobenzene, 1,2-dichlorobenzene, nitrobenzene). Since fullerene can be considered as a Lewis acid,[33,34] enhancement of the electron-donating properties of the solvent is expected to entail a better interaction between the C_{60} and solvent molecules,

which affects the heat of dissolution. The process becomes more exothermic when the solvent molecule has electron-donating groups. This can be clearly followed in the series: benzene, toluene, bromobenzene, 1,2-dichlorobenzene. The researchers cited [33] concluded that the enthalpy of dissolution can also be used to predict the fullerene solubility. Heymann [31] used the Scatchard – Hildebrand model to describe the C_{60} solubility in the series of alkanes, isoalkanes, n-alkanols, isoalkanols and diols; in total, the solubility in 26 solvents was studied. An expression relating the solubility and the parameter δ of the solvent was derived; however, this second order polynomial of the Hildebrand parameter was found to be suitable only for the description of the class of alkanes.

In was noted in a number of papers [22, 23, 27] that the regular solution model is inapplicable to fullerene solutions, as this model considers cases of positive excess enthalpy of dissolution and zero excess entropy of dissolution, whereas the dissolution of fullerenes is exothermic ($\Delta H_{solv} < 0$). The entropy of dissolution is also negative and is often much greater in absolute magnitude than the enthalpy referred to the absolute temperature. Thus, the dissolution of fullerenes is subject to entropy control, which reflects the fact that solvation, unlike destruction of fullerite, causes ordering in the solution.

Semenov *et al.*[35] analyzed the available literature data on the isothermal solubility of individual light fullerenes in organic solvents of various classes (n-alkanes, n-alkanoic acids, n-alkanols, arenes) as a function of the hydrocarbon chain length and found a correlation between the solubility and the Hildebrand parameter of the solvent (Fig. 10). It is pertinent to note several publications on the qualitative estimation and prediction of the solubility of fullerenes in one-component organic solvents and in multicomponent systems (vegetable oils) using the Hansen method.[36] This method is based on elucidation of correlations between components of the Hildebrand solubility parameter for the solvent (dispersive contribution, contribution from hydrogen bonding and contribution of dipole–dipole interactions to the total cohesion energy) and the fullerene solubility. Of special note is the series of works [37 – 41] reporting an approach to elucidating the quantitative structure – property relationships (QSPR model), *i.e.*, the relationship between the fullerene solubility and structural characteristics of the solvents.

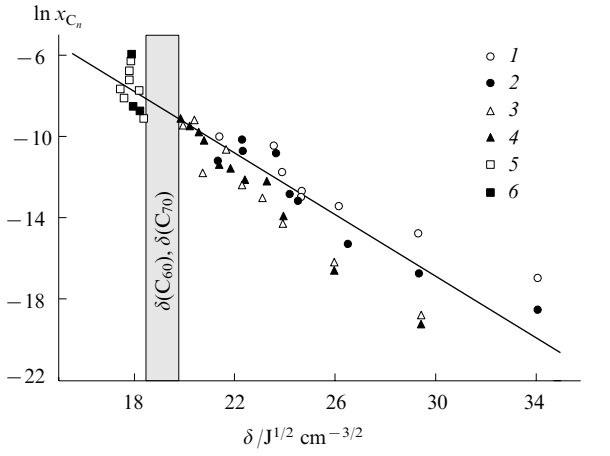


Figure 10. Logarithm of the mole fraction of individual light fullerene (C_{60} or C_{70}) in a saturated solution (at 293 K) *vs.* the Hildebrand solubility parameter of the solvent.[35]
Solubility in n-alkanoic acids $C_nH_{2n+1}CO_2H$ ($n = 1-9$): C_{60} (*1*), C_{70} (*2*); in n-alkanols $C_nH_{2n+1}OH$ ($n = 1-11$): C_{60} (*3*), C_{70} (*4*); in aromatics $Me_nC_6H_{6-n}$ ($n = 1-4$): C_{60} (*5*), C_{70} (*6*).

II.3. Effect of the pressure on the fullerene solubility

Studies of polybaric solubility in systems containing light fullerenes deserve special attention. Only two systems, C_{60} – n-hexane (Table 1) [42] and C_{60} – toluene (Fig. 11),

Table 1. Polybaric solubility of C_{60} in the binary system C_{60} – n-hexane at 298.2 K.[42]

p /MPa	S /g litre^{-1}	p /MPa	S /g litre^{-1}
50	0.102	250	0.256
100	0.165	300	0.281
150	0.213	350	0.290
200	0.230	400	0.324

have been studied to date.[43] Ruelle *et al.*[29] discovered the effect of decreasing molar volume of C_{60} upon dissolution with respect to the solid crystalline phase, which is absolutely untypical of non-electrolytes. In the authors' opinion, in the crystal, the repulsion between the π-orbitals of C_{60}, which propagates in every direction, forces the fullerene molecules to be oriented so as to decrease the repulsion from the environment, which prevents molecules from approaching one another and keeps them at some equilibrium distance. Thus, the decrease in the volume upon dissolution brings about the untypical increase in the solubility with increase in pressure. This fact also follows from the Planck – van Laar equation [30]

$$\left(\frac{\mathrm{d}\ln x_{C_{60}}^{(l)}}{\mathrm{d}p}\right)_T = \frac{\Delta V}{RT} \qquad (8)$$

where ΔV is the change in the molar volume of C_{60} on going from the crystalline form to the saturated solution. Equation (8) holds only in the case of ideal or infinitely dilute

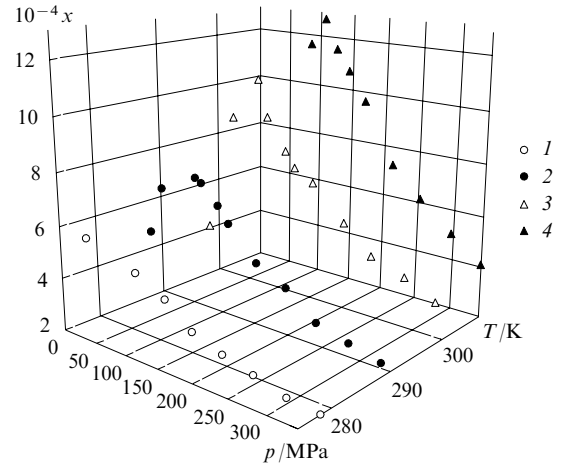


Figure 11. pTx-Diagram for the C_{60} – toluene system.[43]
Temperature /K: 278.2 (*1*), 288.2 (*2*), 298.2 (*3*), 308.2 (*4*).

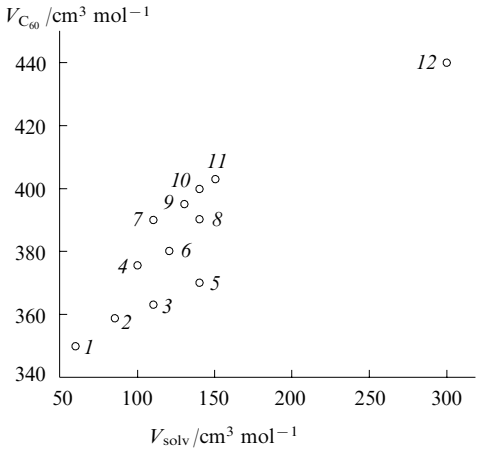


Figure 12. Molar volume of C_{60} in the solution *vs.* molar volume of the solvent.[29]
(*1*) CS_2, (*2*) benzene, (*3*) toluene, (*4*) chlorobenzene, (*5*) 1,2,4-trimethylbenzene, (*6*) *o*-xylene, (*7*) 1,2-dichlorobenzene, (*8*) 1-methylnaphthalene, (*9*) 1,2,4-trichlorobenzene, (*10*) 1-chloronaphthalene, (*11*) *cis*-decalin, (*12*) n-hexadecane.

solutions. Ruelle *et al.*[29] were able to find a correlation between the partial molar volume of C_{60} and the molar volume of the solvent. It was found that the smaller the size of solvent molecules, the more efficiently they occupy the voids between the fullerene molecules in solution, and the smaller the partial molar volume of fullerene in the solution (Fig. 12).

The publication of Sawamura and Fujita[43] deserves special note because it reports for the first time the three-dimensional *pTx* diagram of C_{60} solubility in toluene (see Fig. 11). Adamenko *et al.*[44] carried out *pVT* measurements for a toluene solution of C_{60} and for pure toluene over a broad temperature (313–371 K) and pressure (0.1–103.1 MPa) ranges. In this study, the equation of state was also derived and the changes in the thermodynamic functions (Gibbs energy, enthalpy, entropy and internal energy) upon pressure change were calculated. The changes in the thermodynamic properties of toluene solutions of C_{60} (under isothermal conditions) were described using the empirical Tait equation of state.[30]

II.4. Solubility diagrams of $C_{60}-C_{70}$–solvent ternary systems

The data on solubility of light fullerenes in ternary systems are sparse; only three ternary systems have been studied: two groups of researchers[14,45] working independently investigated the $C_{60}-C_{70}$–*o*-xylene system over a broad temperature range (20–100 °C), while Semenov *et al.*[46,47] presented experimental data and characterized the obtained solubility diagrams for $C_{60}-C_{70}$–styrene and $C_{60}-C_{70}$–1,2-dichlorobenzene systems (Table 2). It is noteworthy that the solubility diagram for the $C_{60}-C_{70}$–*o*-xylene system is relevant for the development of procedures for rough pre-chromatographic separation of fullerenes C_{60} and C_{70}, as the extraction of lower fullerenes from fullerene carbon black is often carried out in a Soxhlet apparatus particularly from *o*-xylene solutions at elevated temperature. In turn, investigation of the $C_{60}-C_{70}$–styrene ternary system is important for the following reasons: it is

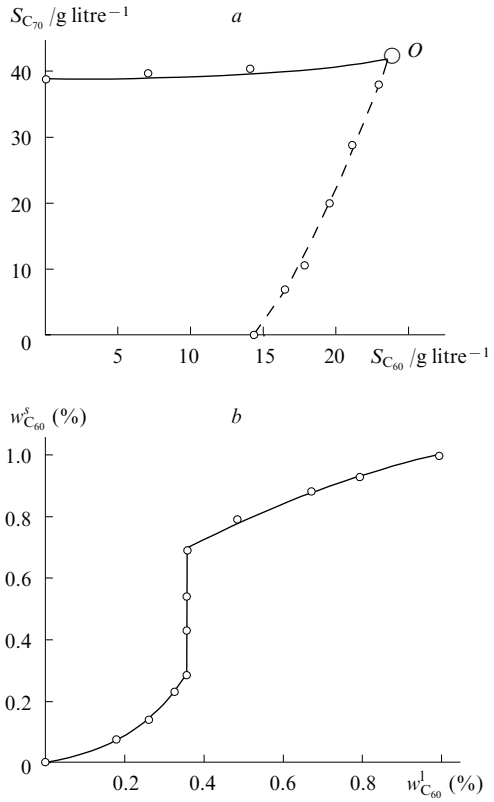


Figure 13. Solubility diagram in the ternary system $C_{60}-C_{70}-1,2\text{-}Cl_2C_6H_4$ at 423 K (*a*) and the diagram of distribution of fullerenes between liquid and solid solutions (*b*).[3]

known from the literature that introduction of individual fullerenes or fullerene mixtures into a solution/melt of a monomer to give a true solution/melt may result, after polymerization, in a new copolymer involving fullerene components.[46,47] Such copolymerization can yield a new polymeric material with enhanced, in some cases quite unique, performance characteristics.[46,47] In this respect, the selection of styrene as the monomer that forms a true solution with light fullerenes at room temperature opens up the way to preparation of a series of new copolymers based on polystyrene, butadiene–styrene rubbers, acrylonitrile–butadiene–styrene resins, *etc.* As an example, consider the solubility diagram of the $C_{60}-C_{70}$–1,2-dichlorobenzene ternary system at 150 °C (Fig. 13 *a*).[1] As can be seen from Fig. 13 *a*, the solubility diagram consists of two branches, the upper one corresponding to crystallization of unsolvated solid solutions enriched with C_{60} and the lower one being due to crystallization of unsolvated solid solutions based on C_{70}. The diagram has one invariant point (point *O* in Fig. 13 *a*) corresponding to simultaneous saturation with both solid phases. The diagram of distribution of the fullerenes between the liquid and solid phases has an area of immiscibility of the components in the solid phase corresponding to the compositions 0.25%–0.7% of fullerene C_{60} in a $C_{60}+C_{70}$ mixture (Fig. 13 *b*).

II.5. Solubility diagrams for the systems individual light fullerene–solvent(1)–solvent(2)

The experimental data devoted to the solubility of individual light fullerenes in a mixture of organic solvents are

Table 2. Compositions of the equilibrium liquid and solid phases in the ternary systems: $C_{60}-C_{70}$–1,2-dimethylbenzene at 253.15, 298.15 and 353.15 K; $C_{60}-C_{70}$–styrene at 258.15, 273.15 and 298.15 K.

$S(C_{60})$ [a]	$S(C_{70})$ [a]	$w^l(C_{60})$ (%)	$w^s(C_{60})$ (%)	Solid phase	$S(C_{60})$ [a]	$S(C_{70})$ [a]	$w^l(C_{60})$ (%)	$w^s(C_{60})$ (%)	Solid phase
		$C_{60}-C_{70}$– 1,2-dimethylbenzene [48]					*$C_{60}-C_{70}$–styrene* [46, 47]		
		T = 353.15 K					T = 298.15 K		
4.44	0.00	1.00	1.00	C_{60}	7.84	2.63	0.75	0.70	$(C_{60})_x(C_{70})_{1-x}\cdot 2\,PhCH{=}CH_2$ (1)
3.78	2.06	0.647	0.950	$(C_{60})_x(C_{70})_{1-x}$ (2)	8.46	3.08	0.73	0.67	$(C_{60})_x(C_{70})_{1-x}\cdot 2\,PhCH{=}CH_2$ (1)
4.15	4.26	0.493	0.900	$(C_{60})_x(C_{70})_{1-x}$ (2)	8.55	4.00	0.64	0.59	$(C_{60})_x(C_{70})_{1-x}$ (2) +
5.26	7.50	0.412	0.850	$(C_{60})_x(C_{70})_{1-x}$ (2)					$(C_{60})_x(C_{70})_{1-x}\cdot 2\,PhCH{=}CH_2$ (1)
6.74	11.18	0.376	0.327	$(C_{60})_x(C_{70})_{1-x}$ (1) + $(C_{60})_x(C_{70})_{1-x}$ (2)	6.03	3.99	0.60	0.50	$(C_{60})_x(C_{70})_{1-x}$ (2)
4.59	11.18	0.291	0.120	$(C_{60})_x(C_{70})_{1-x}$ (1)	4.97	4.02	0.55	0.40	$(C_{60})_x(C_{70})_{1-x}$ (2)
2.15	13.23	0.140	0.045	$(C_{60})_x(C_{70})_{1-x}$ (1)	2.61	4.30	0.39	0.30	$(C_{60})_x(C_{70})_{1-x}$ (2)
0.55	16.76	0.032	0.027	$(C_{60})_x(C_{70})_{1-x}$ (1)	2.07	4.85	0.30	0.20	$(C_{60})_x(C_{70})_{1-x}$ (2)
0.00	21.47	0.000	0.000	C_{70}	1.27	5.25	0.19	0.15	$(C_{60})_x(C_{70})_{1-x}$ (2)
		T = 298.15 K			0.60	6.02	0.09	0.05	$(C_{60})_x(C_{70})_{1-x}$ (2)
9.25	0.00	1.00	1.00	$C_{60}\cdot 2\,(o\text{-}Me_2C_6H_4)$	0.00	6.02	0.00	0.00	C_{70}
9.00	2.40	0.714	0.939	$(C_{60})_x(C_{70})_{1-x}\cdot 2\,(o\text{-}Me_2C_6H_4)$ (2)			T = 273.15 K		
10.54	5.17	0.576	0.912	$(C_{60})_x(C_{70})_{1-x}\cdot 2\,(o\text{-}Me_2C_6H_4)$ (2)	5.50	0.00	1.00	1.00	$C_{60}\cdot 2\,PhCH{=}CH_2$
11.99	7.80	0.506	0.850	$(C_{60})_x(C_{70})_{1-x}\cdot 2\,(o\text{-}Me_2C_6H_4)$ (2)	6.84	1.29	0.84	0.89	$(C_{60})_x(C_{70})_{1-x}\cdot 2\,PhCH{=}CH_2$ (1)
13.11	9.98	0.476	0.407	$(C_{60})_x(C_{70})_{1-x}$ (1) +	7.22	2.17	0.77	0.86	$(C_{60})_x(C_{70})_{1-x}\cdot 2\,PhCH{=}CH_2$ (1)
				$(C_{60})_x(C_{70})_{1-x}\cdot 2\,(o\text{-}Me_2C_6H_4)$ (2)	7.24	2.39	0.76	0.81	$(C_{60})_x(C_{70})_{1-x}\cdot 2\,PhCH{=}H_2$ (1)
9.03	10.34	0.368	0.141	$(C_{60})_x(C_{70})_{1-x}$ (1)	7.69	3.57	0.76	0.74	$(C_{60})_x(C_{70})_{1-x}$ (2) +
3.99	11.12	0.193	0.045	$(C_{60})_x(C_{70})_{1-x}$ (1)					$(C_{60})_x(C_{70})_{1-x}\cdot 2\,PhCH{=}CH_2$ (1)
0.74	13.07	0.036	0.027	$(C_{60})_x(C_{70})_{1-x}$ (1)	5.45	3.79	0.59	0.50	$(C_{60})_x(C_{70})_{1-x}$ (2)
0.00	15.17	0.000	0.000	C_{70}	4.99	4.20	0.54	0.38	$(C_{60})_x(C_{70})_{1-x}$ (2)
		T = 253.15 K			3.84	4.59	0.46	0.32	$(C_{60})_x(C_{70})_{1-x}$ (2)
0.00	4.34	0.000	0.000	$C_{70}\cdot 2\,(o\text{-}Me_2C_6H_4)$	2.53	5.38	0.32	0.23	$(C_{60})_x(C_{70})_{1-x}$ (2)
0.95	3.20	0.230	0.048	$(C_{60})_x(C_{70})_{1-x}\cdot 2\,(o\text{-}Me_2C_6H_4)$ (1)	0	5.60	0.00	0.00	C_{70}
2.39	2.90	0.452	0.110	$(C_{60})_x(C_{70})_{1-x}\cdot 2\,(o\text{-}Me_2C_6H_4)$ (1)			T = 258.15 K		
2.16	4.20	0.509	0.402	$(C_{60})_x(C_{70})_{1-x}\cdot 2\,(o\text{-}Me_2C_6H_4)$ (1) +	5.90	0.00	1.00	1.00	$C_{60}\cdot 2\,PhCH{=}CH_2$
				$(C_{60})_x(C_{70})_{1-x}\cdot 2\,(o\text{-}Me_2C_6H_4)$ (2)	6.41	0.49	0.93	0.86	$(C_{60})_x(C_{70})_{1-x}\cdot 2\,PhCH{=}CH_2$ (1)
3.43	1.75	0.653	0.897	$(C_{60})_x(C_{70})_{1-x}\cdot 2\,(o\text{-}Me_2C_6H_4)$ (2)	7.16	1.23	0.85	0.84	$(C_{60})_x(C_{70})_{1-x}\cdot 2\,PhCH{=}CH_2$ (1)
2.33	0.77	0.751	0.951	$(C_{60})_x(C_{70})_{1-x}\cdot 2\,(o\text{-}Me_2C_6H_4)$ (2)	7.84	2.62	0.75	0.71	$(C_{60})_x(C_{70})_{1-x}\cdot 2\,PhCH{=}CH_2$ (1)
1.81	0.00	1.000	1.000	$C_{60}\cdot 2\,(o\text{-}Me_2C_6H_4)$	8.01	3.56	0.69	0.66	$(C_{60})_x(C_{70})_{1-x}$ (2) +
		$C_{60}-C_{70}$–styrene [46, 47]							$(C_{60})_x(C_{70})_{1-x}\cdot 2\,PhCH{=}CH_2$ (1)
		T = 298.15 K			5.33	2.69	0.66	0.46	$(C_{60})_x(C_{70})_{1-x}$ (2)
4.02	0.00	1.00	1.00	$C_{60}\cdot 2\,PhCH{=}CH_2$	2.97	2.75	0.52	0.37	$(C_{60})_x(C_{70})_{1-x}$ (2)
4.88	0.11	0.98	0.93	$(C_{60})_x(C_{70})_{1-x}\cdot 2\,PhCH{=}CH_2$ (1)	2.01	2.78	0.42	0.26	$(C_{60})_x(C_{70})_{1-x}$ (2)
5.64	0.32	0.95	0.89	$(C_{60})_x(C_{70})_{1-x}\cdot 2\,PhCH{=}CH_2$ (1)	2.01	2.78	0.42	0.26	$(C_{60})_x(C_{70})_{1-x}$ (2)
6.55	0.77	0.90	0.83	$(C_{60})_x(C_{70})_{1-x}\cdot 2\,PhCH{=}CH_2$ (1)	1.35	2.80	0.33	0.17	$(C_{60})_x(C_{70})_{1-x}$ (2)
6.96	1.08	0.87	0.80	$(C_{60})_x(C_{70})_{1-x}\cdot 2\,PhCH{=}CH_2$ (1)	0.31	2.82	0.1	0.09	$(C_{60})_x(C_{70})_{1-x}$ (2)
7.20	1.70	0.80	0.75	$(C_{60})_x(C_{70})_{1-x}\cdot 2\,PhCH{=}CH_2$ (1)	0.00	2.84	0.00	0.00	C_{70}

Note. $S(C_{60})$ is the C_{60} concentration in the solution, $S(C_{70})$ is the C_{70} concentration in the solution, $w^l(C_{60})$ is the mass fraction of C_{60} in the liquid solution, $w^s(C_{60})$ is the mass fraction of fullerene C_{60} in the solid solution; (1), (2) are solid solutions enriched with C_{60} and C_{70}, respectively. [a] In g litre^{-1}.

Table 3. Temperature dependence of the solubility of fullerene C_{60} (x 10^4, x is the mole fraction of C_{60} in the saturated solution) in the mixtures: tetrachloromethane (1) – toluene (2), tetrachloromethane (1) – *o*-dichlorobenzene (2), tetrachloromethane (1) – tetralin (2) and 1,2-dichlorobenzene (1) – tetralin (2).

x_2 (see [a])	T/K					x_2 (see [a])	T/K				
	298.15	308.15	318.15	328.15	338.15		298.15	308.15	318.15	328.15	338.15
	Tetrachloromethane (1) – toluene (2) [49, 50]						*Tetrachloromethane (1) – tetralin* (2) [51, 52]				
0	0.376	0.423	0.401	0.407	0.413	0	0.376	0.423	0.401	0.407	0.413
0.103	0.503	0.510	0.517	0.525	0.532	0.1	1.15	1.6	1.82	2.18	2.49
0.302	0.680	0.831	0.828	0.839	0.793	0.3	7.08	7.84	8.1	11.11	9.27
0.502	1.18	1.25	1.22	1.33	1.33	0.5	15.09	13.36	13.06	12.34	10.83
0.706	1.82	1.77	1.83	1.97	1.75	0.7	23.75	29.51	34.47	28.5	27.86
0.890	2.83	3.07	2.56	2.44	2.32	0.9	23.57	30.26	35.74	41.47	50.05
1	3.61	3.31	3.12	3.00	2.80	1	23.52	20.47	33.36	44.77	50.99
	Tetrachloromethane (1) – 1,2-dichlorobenzene (2) [49, 50]						*1,2-Dichlorobenzene (1) – tetralin (2)* [51, 52]				
0	0.376	0.423	0.401	0.406	0.413	0	42.2	36.3	23.4	19.1	21.9
0.103	0.63	0.693	0.632	0.655	0.692	0.1	47.94	38.86	31.73	28.28	24.54
0.306	1.7	1.8	1.7	1.91	2.15	0.3	63.66	50.39	42.36	38.07	30.92
0.500	4.52	4.72	4.77	5.13	5.34	0.5	63.4	60.38	48.66	48.13	42.67
0.691	9.94	11.7	12.0	12.1	11.1	0.7 [b]	33.44	39.18	45.6	55.72	48.53
0.900	29.3	31.1	18.8	16.0	17.8	0.9 [c]	23.34	32.38	38.59	47.39	57.26
1	42.2	36.3	23.4	19.1	21.9	1	23.52	29.47	33.36	44.77	50.99

[a] Here and in Table 4, x_2 is the mole fraction of solvent (2); [b] $x \times 10^4 = 45.35$ (348.15 K) or 43.57 (358.15 K); [c] $x \times 10^4 = 70.73$ (343.15 K), 56.07 (348.15 K) or 46.16 (358.15 K).

Table 4. Temperature dependence of the solubility of C_{60} ($x \times 10^4$) in the tetrachloromethane (1) – tetralin (2) mixture.[51]

x_2	T/K										
	323.15	333.15	340.15	341.15	343.15	345.15	348.15	353.15	358.15	363.15	368.15
0.3	15.08	–	–	–	–	–	–	–	–	–	–
0.7	41.18	–	–	–	–	–	–	–	–	–	–
0.9	38.20	47.17	–	–	–	–	53.59	47.00	35.69	–	–
1.0	–	–	60.64	81.92	80.12	63.24	58.76	55.84	49.98	39.95	35.49

Table 5. Solubility of C_{60} in [a] decalin (1) – naphthalene (2), toluene (1) – naphthalene (2) and dodecane (1) – naphthalene (2) mixtures.[53]

Decalin (1) – naphthalene (2)		Toluene (1) – naphthalene (2)		Dodecane (1) – naphthalene (2)	
w_2 (%)	S/g litre^{-1}	w_2 (%)	S/g litre^{-1}	w_2 (%)	S/g litre^{-1}
0	1.7	0	2.7	0	0.09
5	2.0	10	3.8	2.5	0.07
10	2.4	15	4.5	5	0.1
15	3.5	20	7.2	6	0.11
		25	7.0	7.8	0.11
		30	7.0	10	0.15
				10.1	0.23

[a] w_2 is the naphthalene content (mass %).

summarized in Table 3 – 7. Studies of fullerene solubility in mixed solvents are of practical interest as the knowledge of a solvation mechanism for fullerenes could serve to perform selective reactions of fullerenes and to develop criteria for the selection of most efficient solvents for separation of fullerene mixtures. We will consider some results obtained along this line. The solubility of C_{60} in CCl_4 – toluene, CCl_4 – 1,2-dichlorobenzene, CCl_4 – tetralin and 1,2-dichlorobenzene – tetralin mixtures has been studied over a broad temperature range (see Tables 3 and 4).[45, 49 – 52] Kolker *et al.*[49, 50] derived the equation describing the dependence of the solubility of C_{60} on the temperature and on the composition of a mixed solvent, estimated the concentration dependence of the Gibbs energy of dissolution and concluded that an increase in the content of the aromatic solvent promotes dissolution, while the temperature has

Table 6. Solubility of C_{60} in the acetonitrile (1) – toluene (2) mixture.[54]

Θ (%) (see [a])	S/g litre^{-1}	Θ, % (see [a])	S/g litre^{-1}
0	0.000	60	0.067
5	0.003	80	0.300
10	0.005	90	0.710
30	0.018	95	0.920
50	0.031	100	2.600

[a] Θ is the volume fraction of toluene.

almost no influence on the process. The formation of crystalline solvates was established for the C_{60} – mixed solvent (CCl_4 – PhMe and CCl_4 – 1,2-$Cl_2C_6H_4$) systems.[49, 50] In the C_{60} – CCl_4 – PhMe system, two crystalline solvates were detected, a low-temperature one (**I**), which incongruently melted in the range from 277.3 to 283 K ($\Delta_r H = 10.3 \pm 0.1$ kJ mol^{-1}), and the second one (**II**) with the incongruent melting point (T_{imp}) and enthalpy ($\Delta_r H$) of 334.0 ± 1.3 K and 11.0 ± 1.9 kJ mol^{-1}, respectively. In the case of the C_{60} – CCl_4 – 1,2-$Cl_2C_6H_4$ system, two solid solvates were also detected: **III**, $T_{imp} = 271.3$ K and $\Delta_r H = 11.1 \pm 0.1$ kJ mol^{-1}; and **IV**, $T_{imp} = 335.5 \pm 0.4$ K and $\Delta_r H = 14.0 \pm 1.6$ kJ mol^{-1}. Kulkarni and Jafvert[55] experimentally studied the solubility of C_{60} in tetrahydrofuran – aceronitrile, toluene – acetonitrile, toluene – tetrahydrofuran and toluene – ethanol mixtures. On the basis of the Hall equation,[57] which relates the excess Gibbs energy of a ternary system to the volume fractions of components with allowance for the difference in the size of molecules forming the solution, they constructed a model describing the dependence of isothermal solubility in a ternary system [C_{60} – solvent(1) – solvent(2)] on the composition of a mixed solvent.

II.6. Phase equilibria of solubility for multicomponent systems containing light fullerenes

The solvents used in this case are mainly biocompatible multicomponent natural phases — vegetable oils, animal fats and essential oils. The solubility of light fullerenes in various fats and oils has not been adequately studied. Apart from the paper[58] reporting the solubility of fullerene C_{60} in olive oil ($\sim$4 – 6 g litre^{-1} depending on temperature), there are only several RF patents[59 – 62] of 2001 – 2006 in which the solubility of light fullerenes in both vegetable and animal fats was estimated only at a qualitative level and, furthermore, the consideration included both true and microheterogeneous (cluster, colloid) solutions of fullerenes. The published data on the solubility of individual light fullerenes and the industrial fullerene mixture in vegetable oils and animal fats are summarized in Tables 8 and 9. Note that data on the fullerene solubility in multicomponent systems can differ several-fold. This is due, first of all, to differences in the oil composition (different contents of tri-, di- and monoglycerides, phospholipids, glycolipids, free fatty acids, sterols, dyes, vitamins, polyphenols, *etc*.) and to different experimental procedures used to study the solubility (for example, in some cases, ultrasonication was employed to saturate the solutions). As a rule, the compositions of the oils used are presented in the original publications. Study of the solubility of light fullerenes in liquid natural vegetable oils and animal fats is topical for a number of reasons. First, fullerenes are rather readily soluble in these natural solvents

Table 7. Solubility of C_{60} in the mixtures toluene (1) – acetonitrile (2), toluene (1) – ethanol (2), toluene (1) – tetrahydrofuran (2), acetonitrile (1) – tetrahydrofuran (2), ethanol (1) – water (2) and tetrahydrofuran (1) – water (2) [Θ_1 is the volume fraction of component (1)].[55, 56]

Ethanol (1) – water (2)		Tetrahydrofuran (1) – water (2)		Toluene (1) – acetonitrile (2)	
Θ_1	S/g litre^{-1}	Θ_1	S/g litre^{-1}	Θ_1	S/g litre^{-1}
0	8.00×10^{-9}	0	8.00×10^{-9}	0	4.37×10^{-5}
					5.16×10^{-5}
					4.24×10^{-5}
					4.61×10^{-5}
0.5	1.18×10^{-6}	0.5	1.23×10^{-5}	0.3	2.39×10^{-3}
	1.45×10^{-6}		2.73×10^{-5}		2.41×10^{-3}
0.6	4.96×10^{-6}	0.6	8.98×10^{-5}	0.5	0.0222
	4.97×10^{-6}		9.36×10^{-5}		0.0215
0.7	2.89×10^{-5}	0.7	3.15×10^{-4}	0.7	0.244
	2.41×10^{-5}		3.18×10^{-4}		0.284
0.8	7.07×10^{-5}	0.8	1.02×10^{-3}	0.9	1.11
	7.32×10^{-5}				1.09
0.9	4.51×10^{-4}	0.9	3.06×10^{-3}	1	3.09
	4.41×10^{-4}		3.32×10^{-3}		2.96
1	1.74×10^{-3}	1	1.14×10^{-2}		
	1.43×10^{-3}		1.08×10^{-2}		

Toluene (1) – ethanol (2)		Acetonitrile (1) – tetrahydrofuran (2)		Toluene (1) – tetrahydrofuran (2)	
Θ_1	S/g litre^{-1}	Θ_1	S/g litre^{-1}	Θ_1	S/g litre^{-1}
0	2.00×10^{-3}	0	4.70×10^{-5}	0	0.0116
			4.30×10^{-5}		0.0111
			3.70×10^{-5}		
0.1	2.79×10^{-3}	0.1	1.10×10^{-4}	0.05	0.0111
	3.04×10^{-3}		9.40×10^{-5}		0.0106
0.3	0.0237	0.15	4.70×10^{-5}	0.1	0.0145
	0.0232				0.0141
0.5	0.124	0.2	6.60×10^{-5}	0.15	0.0138
	0.121		4.90×10^{-5}		0.0136
0.7	0.494	0.25	6.70×10^{-5}	0.2	0.0174
	0.542				0.0166
0.9	1.38	0.4	1.60×10^{-4}	0.3	0.0217
	1.38		1.20×10^{-4}		0.0144
1	3.00	0.5	2.80×10^{-4}	0.35	0.0245
					0.0241
		0.6	5.70×10^{-4}	0.50	0.0458
			6.10×10^{-4}		0.0463
		0.75	1.59×10^{-3}	0.6	0.0660
			1.61×10^{-3}		0.0641
		0.8	2.57×10^{-3}	0.65	0.0890
			3.08×10^{-3}		0.0957
		0.9	5.59×10^{-3}	0.7	0.104
			6.40×10^{-3}		0.130
		1	0.0111	0.75	0.180
			0.0105		0.160
				0.8	0.323
					0.284
				0.9	1.23
					1.18
				1	3.09
					2.96

Table 8. Solubility (S/g litre^{-1}) of fullerenes in vegetable oils.

Solvent	T/K					Ref.
	273.15	293.15	313.15	333.15	353.15	
			Fullerene C_{60}			
Stavropolye (unrefined sunflower oil)	0.294	0.451	0.727	0.708	0.638	63
Zlato (refined sunflower oil)	0.299	0.377	0.456	0.570	0.697	63
Sunflower oil	–	0.116	–	–	–	64
	–	0.522	–	–	–	65
Venus (sunflower oil)	–	6.91	–	–	–	58
Floriol (sunflower oil)	–	4.01	–	–	–	58
Eden (sunflower oil)	–	5.62	–	–	–	58
Milora (corn oil)	0.196	0.609	0.846	0.945	1.319	63
Walnut oil	0.269	0.485	0.694	0.718	1.017	63
Olive oil	0.264	0.470	0.751	0.858	1.206	63
	5.99 (283.15 K)	4.61 (303 K)	3.88 (313 K)			58
	–	0.909	–	–	–	65
	–	–	23.6 [a] (323 K)	–	–	66
	–	0.173	–	–	–	64
Carapelli (olive oil)	–	2.84	–	–	–	58
Borgess (olive oil)	–	5.97	–	–	–	58
Olatalia (olive oil)	–	3.97	–	–	–	58
Linseed oil	0.229	0.513	0.639	0.717	1.033	63
	–	0.365	–	–	–	65
	–	–	–	53.1 [a] (328 K)	–	66
	–	0.091	–	–	–	64
Pine nut oil	0.323	0.485	0.818	1.053	1.099	63
	–	–	–	51.8 [a] (343 K)	–	66
Grape-kernel oil	0.327	0.371	0.663	0.748	0.897	63
Apricot kernel oil	0.372	0.509	0.702	0.799	0.958	63
Biodiesel	–	0.187	–	–	–	64
	–	0.859	–	–	–	65
Soybean oil	–	0.134	–	–	–	64
	–	0.495	–	–	–	65
Castor oil	–	0.392	–	–	–	65
Nut oil	–	0.751	–	–	–	65
Sea buckthorn oil	–	–	–	43.2 [a] (328 K)	–	66
			Fullerene C_{70}			
Stavropolye (unrefined sunflower oil)	0.504	1.827	2.647	2.872	3.213	28
Zlato (refined sunflower oil)	0.303	1.289	1.668	2.996	3.261	28
Sunflower oil	–	0.867	–	–	–	64
Milora (corn oil)	0.506	1.957	2.963	3.404	4.286	28
Walnut oil	0.315	1.390	1.829	2.650	2.837	28
Olive oil	0.402	0.756	1.286	2.735	3.278	28
	–	1.035	–	–	–	64
Linseed oil	0.505	1.198	1.639	2.118	2.773	28
	–	0.727	–	–	–	64
Pine nut oil	0.378	0.757	1.512	2.020	2.710	28
Grape-kernel oil	0.632	0.947	1.578	2.207	2.838	28
Apricot kernel oil	0.378	1.009	2.208	2.772	3.090	28
Castor oil	–	0.636	–	–	–	64
Nut oil	–	0.852	–	–	–	64
Soybean oil	–	0.753	–	–	–	64
Cabbage oil	–	1.034	–	–	–	64

Table 8 (continued).

Solvent	T/K					Ref.
	273.15	293.15	313.15	333.15	353.15	
Fullerene mixture: 60% – 65% C_{60} + 33% – 39% C_{70} + 1% – 2% C_{76-90} (see [b])						
Stavropolye (unrefined sunflower oil)	1.831	2.234	2.068	1.839	1.612	63
	0.898	1.045	1.361	1.843	2.320	63
Zlato (refined sunflower oil)	1.828	2.284	2.510	2.663	2.864	63
	1.279	1.456	1.731	1.825	2.199	63
Milora (corn oil)	1.949	2.294	2.746	2.619	2.735	63
	1.209	1.201	1.346	1.664	1.976	63
Walnut oil	1.378	2.127	2.156	2.264	2.340	63
	0.752	0.890	1.362	1.517	1.546	63
Olive oil	1.239	2.900	2.224	2.135	2.150	63
	0.913	1.123	1.518	1.747	1.999	63
Linseed oil	1.733	2.097	2.067	1.987	1.923	63
	0.900	1.117	1.207	1.524	1.778	63
Pine nut oil	1.711	2.026	2.479	2.484	2.607	63
	1.370	1.681	1.826	2.079	2.294	63
Grape-kernel oil	1.693	1.801	2.092	2.263	2.224	63
	1.059	1.214	1.301	1.517	1.675	63
Apricot kernel oil	1.437	1.791	1.905	2.086	2.097	63
	0.908	1.056	1.463	1.487	1.553	63

[a] Fullerene solutions were saturated using an ultrasonic unit. [b] The upper value corresponds to the solubility of fullerene C_{60} from the fullerene mixture; the lower value is the solubility of fullerene C_{70} from the fullerene mixture.

Table 9. Solubility of light fullerenes in animal fats (g litre^{-1}).

Solvent	T/K				Ref.
	323.15	333.15	343.15	353.15	
		Fullerene C_{60}			
Pork fat	0.052	0.145	0.231	0.257	67
Chicken fat	0.024	0.059	0.093	0.122	67
Beef fat	0.041	0.131	0.153	0.168	67
Margarine 'Rumyashka'	–	0.019	0.028	0.029	67
Lamb fat	0.041	0.212	0.385	0.541	67
Cow butter	0.021	0.046	0.063	0.087	67
Molten cow butter	Soluble				68
Cod liver oil	–	53.0 [a] (338 K)	–	–	5
		Fullerene C_{70}			
Pork fat	0.143	0.291	0.529	0.582	67
Chicken fat	0.148	0.344	0.661	0.688	67
Beef fat	0.054	0.096	0.134	0.160	67
Margarine 'Rumyashka'	–	0.080	0.132	0.252	67
Lamb fat	0.053	0.132	0.238	0.317	67
Cow butter	0.159	0.360	0.556	0.587	67
Molten cow butter	Soluble				65
		Fullerene mixture 65% C_{60} + 34% C_{70} + 1% C_{76-90} (see [b])			
Pork fat	0.109	0.437	0.649	0.650	67
	0.184	0.381	0.571	0.670	
Chicken fat	0.195	0.401	0.533	0.571	67
	0.191	0.284	0.428	0.495	
Beef fat	0.126	0.226	0.521	0.551	67
	0.045	0.190	0.477	0.476	
Margarine	–	0.021	0.135	0.199	67
	–	0.098	0.193	0.240	

Table 9 (continued).

Solvent	T/K				Ref.
	323.15	333.15	343.15	353.15	
	Fullerene mixture 65% C_{60} + 34% C_{70} + 1% C_{76-90} (see [b])				
Lamb fat	0.058	0.282	0.409	0.512	67
	0.194	0.306	0.460	0.546	
Cow butter	0.177	0.261	0.354	0.426	67
	0.154	0.258	0.309	0.368	

[a, b] See Table 8.

Table 10. Solubility of light fullerenes in essential oils.[5, 69]

Solvent	T/K						
	293.15	303.15	313.15	323.15	333.15	343.15	353.15
	Fullerene C_{60}						
Clove oil	1.551	1.778	2.168	2.880	3.011	3.275	3.864
Lemon oil	–	–	–	18.8 [a]	–	–	–
Orange oil	–	–	–	21.3 [a] (329 K)	–	–	–
Cypress oil	–	–	–	20.6 [a]	–	–	–
Eucalyptus oil	–	–	–	23.4 [a] (328 K)	–	–	–
Terpentine oil	–	–	–	–	25.6 [a] (338 K)	–	–
Fullerene C_{70}							
Clove oil	0.906	1.026	1.267	1.715	2.037	2.662	5.619
	Fullerene mixture 65% C_{60} + 34% C_{70} + 1% C_{76-90} (see [b])						
Clove oil	3.554	3.544	3.576	3.622	4.057	4.631	7.095
	1.742	1.962	2.108	2.107	2.448	2.463	2.897
Juniper oil (wood)	3.068	3.205	3.520	4.441	5.403	5.530	5.677
	3.223	3.586	4.239	5.022	5.731	6.315	6.458
Juniper oil (leaves)	2.872	2.956	3.506	3.793	4.136	4.337	4.348
	3.196	3.278	3.682	4.094	3.246	2.654	2.402

[a, b] See Table 8.

in this temperature range — from tenths to a few grammes of fullerenes per litre of the solution (see Tables 8 and 9).[5, 32, 58, 63–67, 69, 70] In natural vegetable oils, fullerenes form time-stable absolutely transparent true solutions. These solutions are harmless and compatible with animal and human bodies if they are prepared directly by extraction of a fullerene mixture from a fullerene carbon black into natural vegetable oils, *i.e.*, virtually no hazardous impurity components are present.[5, 58, 63–67, 69]

Standard fullerenes obtained, as a rule, from solutions in aromatic solvents (toluene, xylenes, dichlorobenzenes, *etc.*) always contain traces of these solvents. Even drying for many hours at 200–250 °C in a fairly high vacuum (0.01 m Hg) retains thousandths to hundredths of a mass percent of residual solvents. An alternative way for complete purification from traces of solvents is apparently only high-temperature vacuum sublimation of fullerenes at very low residual pressures ($< 10^{-5}$ mm Hg). Experience shows that this process is fairly expensive and labour-consuming; therefore, the price of so-called sublimed fullerene C_{60} free from solvent impurities is 2–4 times higher than the price of conventional fullerene C_{60} obtained by the standard drying procedure in a vacuum chamber. Second, solutions of fullerenes in oil (fat) possess strong antibacterial and antioxidant properties; they can absorb free radicals and radical ions from condensed phases in which they occur and can absorb photons in the UV spectral region (see, for example, monographs [17, 34, 65]); this could undoubtedly find practical application.[17, 28, 34, 58, 63–65, 67]

The solubility of individual fullerenes and a standard fullerene mixture (65% C_{60}, 34% C_{70}, 1% C_{76-90}) in the so-called wood essential oils, in particular, juniper (leaves), juniper (wood) and clover oils was investigated [5, 69] in the temperature range of 0–80 °C (Table 10). The fullerene additives were found to serve as efficient odour stabilizers.

III. Extraction equilibria in systems containing light fullerenes

This Section is devoted to descriptions of two-phase liquid(1)–liquid(2) equilibria in systems containing light fullerenes and to verification of the possibility to use extraction for separation and purification of particular fullerene. The extraction equilibria have now been studied

for the following systems: $C_{60}-C_{70}-o$-xylene – isobutylamine – H_2O,[71] $C_{60}-C_{70}-o$-xylene – monoethanolamine,[72] $C_{60}-C_{70}-o$-xylene – DMF – H_2O,[72] $C_{60}-C_{70}$ – toluene – DMF – H_2O,[73] $C_{60}-C_{70}-\alpha$-pinene – ethanol – H_2O,[74] $C_{60}-C_{70}-o$-xylene – ethanol – H_2O[73] and $C_{60}-C_{70}$ – 1,2,4-trichlorobenzene – ethanol – H_2O.[75] In all cases, the extraction equilibria were studied at 25 °C. While choosing the extraction systems, the researchers cited [71–75] were guided by the following criteria.

1. The phase diagram for the major components of the system (solvents) should have a broad concentration range of immiscibility, so that the physicochemical properties of the coexisting phases be considerably different and one could reasonably assume that the distribution constants of fullerenes between the phases would be rather high.

2. For engineering purposes, it is necessary that the solubility of C_{60} and C_{70} in both coexisting phases be significant (at least 50 – 100 mg of fullerenes in 1 litre of the solution).

3. It is desirable that the solvents should not chemically react with the dissolved fullerenes and should not form, for example, charge transfer complexes, which is the case with anthracene.[27] In any case, the formation reactions of such compounds should be reversible or these compounds should easily decompose to give pure fullerenes. Analysis of published data on the solubility of C_{60} and C_{70} in individual solvents (see Table 1 of the electronic supplement) indicates that the range of suitable compounds is rather narrow. This can be an aromatic compound (benzene, toluene, a xylene or halobenzene, naphthalene, anthracene, phenanthrene, heterocyclic compound, *e.g.*, pyridine, and some other), CS_2, CCl_4, CHI_3, some amines, decalin and other not abundant compounds. Analysis of the reference data on liquid(1) – liquid(2) phase equilibria demonstrates that the vast majority of pairs of components taken from the above list are miscible at about the room temperature in any ratios; even if phase separation is possible (*e.g.*, in anthracene-containing systems at elevated temperature), too strong compounds of fullerenes with the solvents are irreversibly formed almost in all cases. We will briefly consider the relevant results.

III.1. The system $C_{60}-C_{70}-o$-xylene – isobutylamine – H_2O

Figure 14 shows the equilibrium diagram of distribution of fullerenes C_{60} and C_{70} between the amine and *o*-xylene phases for four-component systems $C_{60}-o$-xylene – isobutylamine – H_2O and $C_{70}-o$-xylene – isobutylamine – H_2O and five-component system $C_{60}-C_{70}-o$-xylene – isobutylamine – H_2O at 25 °C.[71] The content of the major components — *o*-xylene, isobutylamine and H_2O — was set constant in the diagrams as well as the overall composition of the C_{60} and C_{70} mixture in the five-component system. The distribution diagrams thus obtained proved to be unexpectedly simple, in particular, rectilinear over the whole concentration range covered (the fullerene concentrations varied almost 100-fold). The C_{60} and C_{70} distribution constants (the concentration ratio between the *o*-xylene and amine phases) proved to be invariable and approximately equal for all of the three systems: $K_{part} \approx 16 \pm 5$ irrespective of whether only one fullerene or both fullerenes were present in the solution (*i.e.*, no competition between the fullerenes was noticed, the fullerenes being extracted independently of each other). Since the extraction distribution constants are equal for C_{60} and C_{70}, it is thus impossible to separate them by extraction in the $C_{60}-C_{70}-o$-xylene – isobutylamine – H_2O system.

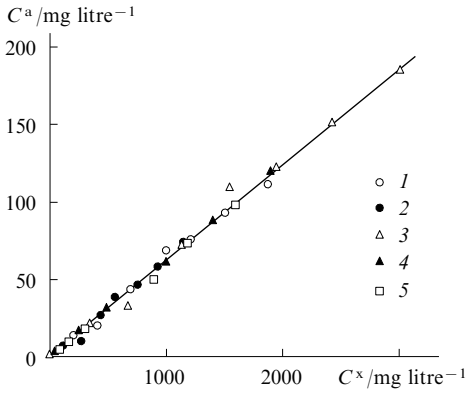


Figure 14. Equilibrium diagram of distribution of C_{60} and C_{70} between the amine (C^a) and *o*-xylene (C^x) phases in the systems: $C_{60}-o$-xylene – isobutylamine – H_2O, $C_{70}-o$-xylene – isobutylamine – H_2O and $C_{60}-C_{70}-o$-xylene – isobutylamine – H_2O at 25 °C.[71] Distribution constants of C_{60} (*1*), C_{70} (*2*), $C_{60}+C_{70}$ (*3*) in the system $C_{60}-C_{70}-o$-xylene – isobutylamine – H_2O; C_{60} (*4*) in the system $C_{60}-o$-xylene – isobutylamine – H_2O; C_{70} (*5*) in the system $C_{70}-o$-xylene – isobutylamine – H_2O.

III.2. The system $C_{60}-C_{70}-o$-xylene – monoethanolamine

Figure 15 presents the diagrams of distribution of fullerenes C_{60} and C_{70} between the monoethanolamine and xylene phases for the four-component system $C_{60}-C_{70}-o$-xylene – monoethanolamine at 25 °C.[72] Figure 16 shows the dependence of the relative mass fractions of C_{60} (in the $C_{60}+C_{70}$ mixture) in the coexisting phases on the C_{70} concentration in the monoethanolamine phase. For clarity, the dashed line designates the overall composition of the fullerene mixture, which contains 46.5 mass % C_{60}. At any concentration, the monoethanolamine phase was enriched with both fullerenes with respect to the *o*-xylene phase. The distribution constants of fullerenes between these phases were always noticeably higher than unity. It can be seen

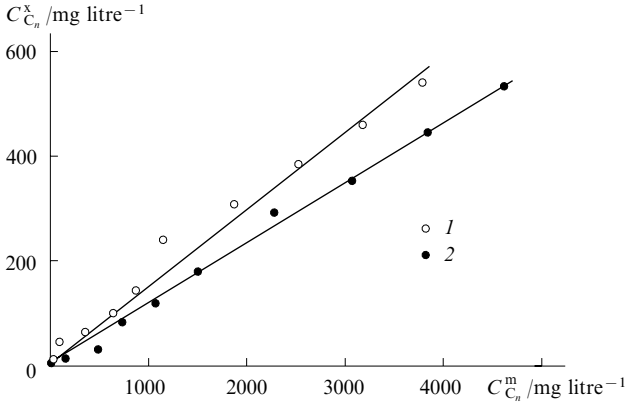


Figure 15. Distribution diagrams of fullerenes C_{60} (*1*) and C_{70} (*2*) between the monoethanolamine (C^m) and *o*-xylene (C^x) phases in the system $C_{60}-C_{70}-o$-xylene – monoethanolamine at 25 °C.[72]

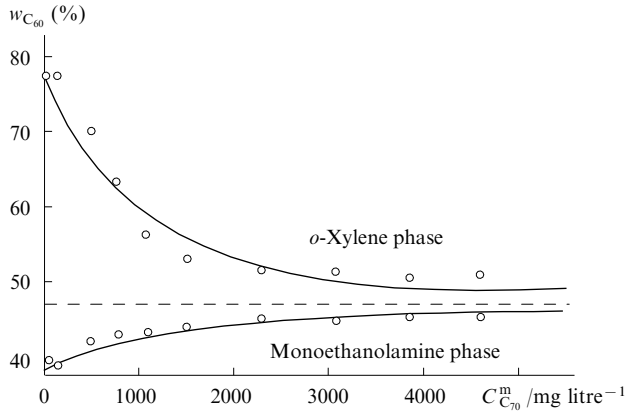


Figure 16. Relative mass fractions of C_{60} (in the $C_{60}+C_{70}$ mixture) in the coexisting phases *vs.* concentration of C_{70} in the monoethanolamine phase in the system $C_{60}-C_{70}-o$-xylene – monoethanolamine at 25 °C (the dashed line shows the overall composition of the fullerene mixture distributed between the phases: 46.5 mass % C_{60}).[72]

from Fig. 15 that the distribution constants for C_{60} increase monotonically with increase in the concentration from ~2 (dilute solutions with a total concentration of fullerenes in the monoethanolamine phase <100 mg litre^{-1}) to ~7 (concentrated solutions with a maximal total concentration of 8400 mg litre^{-1}). Conversely, the distribution constants of C_{70} increase monotonically with increase in the concentration from 12 (dilute solutions) to 8.5 (concentrated solutions). It follows from Fig. 16 that as the total concentration of fullerenes increases, the relative mass fractions of C_{60} (in the a $C_{60}+C_{70}$ mixture) in the coexisting phases gradually approach the overall composition of the mixture distributed between the phases (46.5 mass % C_{60}), which is shown by a dashed line in the Figure. Whereas in dilute (regarding fullerenes) solutions, C_{70} predominantly (compared with C_{60}) passes into the monoethanolamine phase, while C_{60}, conversely, goes into the *o*-xylene phase, in concentrated solutions, this effect is leveled off; the relative content of fullerene C_{60} (in the $C_{60}+C_{70}$ mixture) becomes the same in both phases, being roughly equal to the overall composition of the fullerene mixture. In other words, it can be said that the specific phase distribution between C_{60} and C_{70} disappears with increaseing concentration. It can be clearly seen in Fig. 16 that an efficient separation of fullerenes of the mixture can be attained only in relatively dilute solutions with a total fullerene concentration <2000 mg litre^{-1}, the best result being observed at even lower concentrations, namely, <500 mg litre^{-1} or even 100 mg litre^{-1}. However, the use of very dilute solutions for separation is disadvantageous because of labourious procedure, high consumption of solvents and high energy expenditure for evaporation of the obtained solutions of fullerenes. At high concentrations (>2000 mg litre^{-1}), separation is also inefficient because of rather low relative enrichment factors. Therefore, the authors consider 500 ± 200 mg litre^{-1} to be the concentration range of choice for the separation of C_{60} and C_{70} mixtures of averaged composition (20 mass % to 80 mass % C_{60} in the $C_{60}+C_{70}$ mixture).

III.3. The system $C_{60}-C_{70}-o$-xylene – dimethylformamide – H_2O

Figures 17 and 18 show the distribution diagrams for fullerenes C_{60} and C_{70} between DMF and *o*-xylene in the five-component system $C_{60}-C_{70}-o$-xylene – DMF – H_2O at 25 °C.[72] The overall composition of the C_{60} and C_{70} mixture was set constant (78 mass % C_{60}). The distribution diagrams for C_{60} and C_{70} were curvilinear over the whole concentration range studied; the curvature of the distribution diagram proved to be much more pronounced for fullerene C_{70} than for C_{60}, and the *o*-xylene phase was always enriched in both fullerenes compared with the DMF phase. The distribution constant (concentration ratio between *o*-xylene and DMF) of C_{60} changes little with concentration, being ~200 (see Fig. 17). The distribution constant of C_{70} changes with concentration to a much greater extent; in particular, it increases monotonically from 1 (for dilute solutions with <20 mg litre^{-1} of C_{70} in the *o*-xylene phase) to 4 (for concentrated solutions with >200 mg litre^{-1} of C_{70} in the *o*-xylene phase) (see Fig. 17). It is of prime importance that the relative enrichment factor (K_{enrich}), equal to the ratio of the distribution constants of

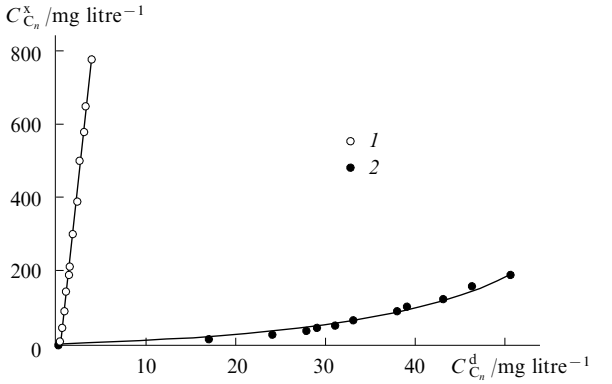


Figure 17. Distribution diagrams of fullerenes C_{60} (*1*) and C_{70} (*2*) between the DMF (C^{d}) and *o*-xylene (C^{x}) phases in the system $C_{60}-C_{70}-o$-xylene – DMF – H_2O at 25°C.[72]

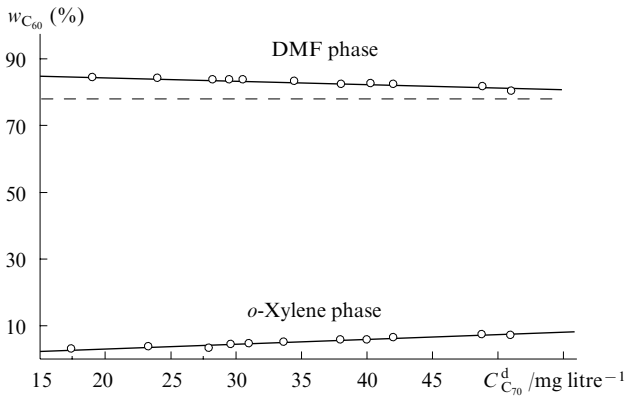


Figure 18. Relative mass fractions of C_{60} (in the $C_{60}+C_{70}$ mixture) in the coexisting phases *vs.* concentration of C_{70} in DMF (C^{d}) in the system $C_{60}-C_{70}-o$-xylene – DMF – H_2O at 25 °C (the dashed line shows the overall composition of the fullerene mixture distributed between the phases: 78.0 mass % C_{60}).[72]

C_{60} and C_{70} is very high, $50 < K_{enrich} < 250$ in the concentration range considered, which provides good opportunities for phase separation. Indeed, the *o*-xylene phase mainly accumulates C_{60} (its concentration ranges from 80 mass % to 84 mass %), whereas DMF contains mainly C_{70} (its concentration is from 92 mass % to 97 mass %). It follows from Figs 17 and 18 that the best separation is achieved in dilute solutions, although it is still quite efficient in relatively concentrated solutions. According to the assumption of Arapov *et al.*,[72] the maximum concentrations corresponding to a total fullerene content of 800 – 1000 mg litre^{-1} are optimal for separation of C_{60} and C_{70}. The total concentration of fullerenes in solution cannot be increased to markedly exceed this value, because deposition of a solid phase immediately starts in DMF and the extraction equilibrium is thus violated. The researchers cited [72] emphasize that the system in question is in principle suitable for some engineering applications: (1) for fast isolation of relatively pure fullerene C_{70} (> 92 mass % purity) for 50 mg litre^{-1} concentration in the solution; (2) for efficient purification of solutions of fullerene C_{60} (up to concentrations of 99 mass % and even higher) for ~1000 mg litre^{-1} concentration in the solution. The authors also pointed out the possibility of extractive isolation of both fullerenes (C_{60} and C_{70}) by so-called extraction cascade consisting of 4 – 5 successive stages.

III.4. The system $C_{60} - C_{70}$ – toluene – dimethylformamide – H_2O

Figures 19 and 20 show the distribution diagrams of fullerenes C_{60} and C_{70} between the DMF and toluene phases for the five-component system $C_{60} - C_{70}$ – toluene – DMF – H_2O at 25 °C.[73] The overall composition of the C_{60} and C_{70} mixture was set constant (76 mass % C_{60}). The distribution diagrams for C_{60} and C_{70} proved to be virtually rectilinear over the whole concentration range. This fact may be attributable to the relatively low concentration range attained in the work (4 times lower for the toluene phase than for the *o*-xylene phase). The highest total concentrations of fullerenes in the toluene phase were ~240 mg litre^{-1} (*vs.* ~1000 mg litre^{-1} in the *o*-xylene phase). As previously, the aromatic (toluene) phase was always enriched in both fullerenes compared with the DMF phase. The distribution constants (the ratios of the concentration in the toluene phase to the concentration in the DMF phase) were 8.1 ± 0.5 for C_{60} and 1.8 ± 0.2 for C_{70} (see Fig. 19). These constants for C_{60} proved to be much lower than for the *o*-xylene system (200), while for C_{70} they were comparable: with increase in the concentration, the distribution constants monotonically increased from 1 to 4. The relative enrichment factor equal to the ratio of the distribution constants of C_{60} and C_{70} proved to be fairly high, namely, 4.5 ± 0.8 in the considered concentration range. This provides good opportunities for phase separation, although they are certainly less favourable than in the *o*-xylene system for which the enrichment factors were $50 < K_{enrich} < 250$. The toluene phase mainly accumulated C_{60} (its relative concentration was 77% to 83%), whereas in DMF, the content of C_{70} increases (its concentration being from 49% to 55%) (see Fig. 19). While comparing this system with the *o*-xylene system, one can note that the separation is much less efficient. Indeed, in the *o*-xylene phase with similar current concentration, C_{60} was predominantly accumulated (80% – 84%), whereas the DMF phase collected mainly C_{70} (however, its relative concentration was much higher, 92 mass % – 97 mass %). Thus, the system in question can in principle be used to separate C_{60} and C_{70}, although it is much inferior to the system $C_{60} - C_{70}$ – *o*-xylene – DMF – H_2O for engineering applications as regards both the purity of isolated fullerenes at the same concentrations and the length of the extraction cascade in the multistage extractive separation.

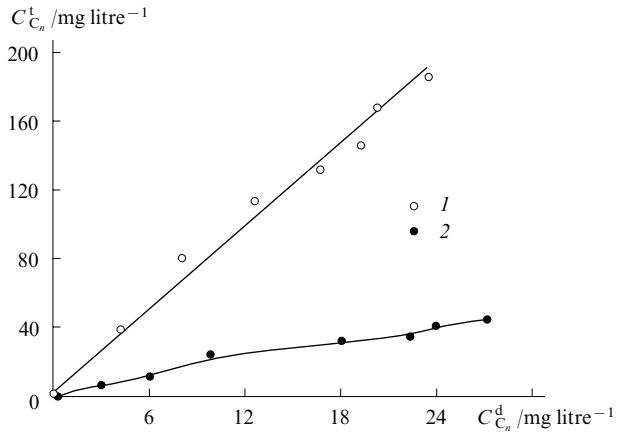


Figure 19. Distribution diagrams of fullerenes C_{60} (*1*) and C_{70} (*2*) between the DMF (C^d) and toluene (C^t) phases in the system $C_{60} - C_{70}$ – toluene – DMF – H_2O at 25 °C.[73]

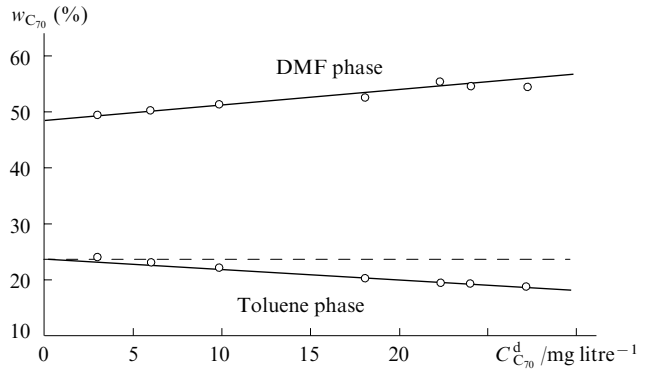


Figure 20. Relative mass fractions of C_{70} (in the $C_{60} + C_{70}$ mixture) in the coexisting phases *vs.* concentration of C_{70} in DMF in the system $C_{60} - C_{70}$ – toluene – DMF – H_2O at 25 °C (the dashed line shows the overall composition of the fullerene mixture distributed between the phases: 24.0 mass % C_{70}).[73]

III.5. The system $C_{60} - C_{70}$ – α-pinene – ethanol – H_2O

Figures 21 and 22 show the diagrams of distribution of fullerenes C_{60} and C_{70} between the α-pinene and ethanol phases for the four-component system $C_{60} - C_{70}$ – α-pinene – ethanol at 25 °C.[74] The overall composition of the mixture of fullerenes C_{60} and C_{70} was set constant (68 mass % C_{60}). The maximal total concentrations of fullerenes in the α-pinene phase were 1400 mg litre^{-1} and those in the ethanol phase were 60 mg litre^{-1} (this is somewhat higher than these values for the DMF-containing systems and lower compared with isobutylamine- and monoethanolamine-containing systems). The α-pinene phase was always

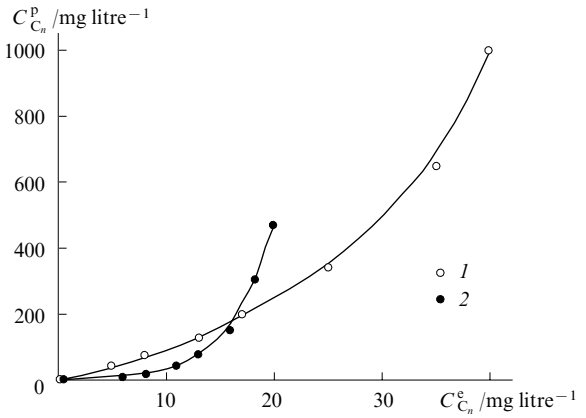


Figure 21. Distribution diagrams of fullerenes C_{60} (*1*) and C_{70} (*2*) between the ethanol (C^{e}) and α-pinene (C^{p}) phases in the system $C_{60}-C_{70}-$ethanol–α-pinene at 25 °C.[74]

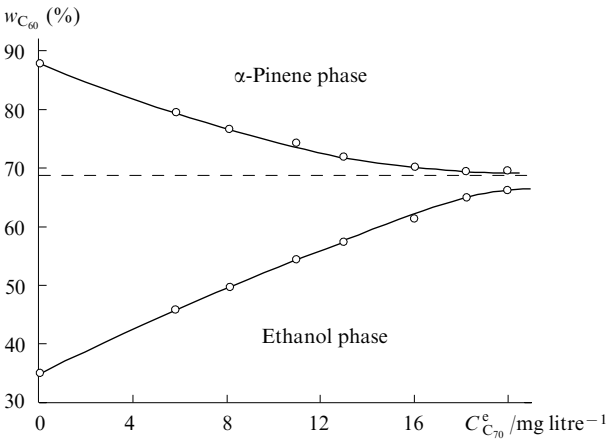


Figure 22. Relative mass fractions of C_{60} (in the $C_{60}+C_{70}$ mixture) in the coexisting phases *vs.* concentration of C_{70} in ethanol (C^{e}) in the system $C_{60}-C_{70}-$ethanol–α-pinene at 25 °C (the dashed line shows the overall composition of the fullerene mixture distributed between the phases: 68 mass % C_{60}).[74]

enriched in both fullerenes relative to the ethanol phase, except for very dilute solutions of C_{70}. The distribution constant (concentration ratio between α-pinene and ethanol phases) of C_{60} increases monotonically from 6.7 for dilute solutions (with the total concentration of fullerenes in α-pinene of 40 mg litre^{-1}) to 25 for concentrated solutions (with the total fullerene concentration in the solution >1400 mg litre^{-1}). The distribution constant of C_{70} varies in parallel, *viz.*, increases monotonically from 0.8 (for dilute solutions) to 2.0 (for concentrated solutions). The relative enrichment factor of C_{60} (the ratio of the distribution constants of C_{60} and C_{70}) monotonically changes to a minor extent from 8.4 (for dilute solutions) to 12.5 (for concentrated solutions); these values are 2–3 times higher than the corresponding values for the toluene system ($K_{enrich} \approx 4.5 \pm 0.8$) and substantially lower than those for the *o*-xylene system ($50 < K_{enrich} < 250$). The α-pinene phase mainly accumulates C_{60} (its relative concentration ranges from 68% to 87%), whereas the ethanol phase contains an increasing amount of C_{70} (its concentration is from 35% to 64%) (see Fig. 22). While comparing this and *o*-xylene systems, one can note much less efficient separation in the former case; when compared with the toluene system, the present system is much more efficient.

III.6. The system $C_{60}-C_{70}-$o-xylene–ethanol–H_2O

Figure 23 shows the dependence of the concentrations of C_{60} and C_{70} in ethanol and *o*-xylene for the system $C_{60}-C_{70}-$*o*-xylene–ethanol–H_2O at 25 °C on the total content of H_2O in the heterogeneous system (the fullerene mixture distributed between the phases contains 83% C_{60}).[73] It should be noted, however, that, since minor amounts of solid mixed fullerene solvates can precipitate from the solution, the actual composition of the mixture distributed between the phases differs somewhat from the above value. The same accounts for a rather strange pattern of the dependence of C_{60} and C_{70} concentrations in *o*-xylene on the total content of water. Indeed, an increase in the total content of water brings about the following changes in the *o*-xylene phase: (a) increase in the content of water (this, undoubtedly reduces the total solubility of fullerenes in this phase and causes precipitation of fullerene solvates); (b) decrease in the ethanol content (this, conversely, increases the concentration of fullerenes; (c) decrease in the fullerene content in the ethanol phase (considering the mass balance, this increases the fullerene content in the *o*-xylene phase). The interplay of all these factors determines the unusual pattern of dependence of the fullerene content in the *o*-xylene phase on the total content of water.

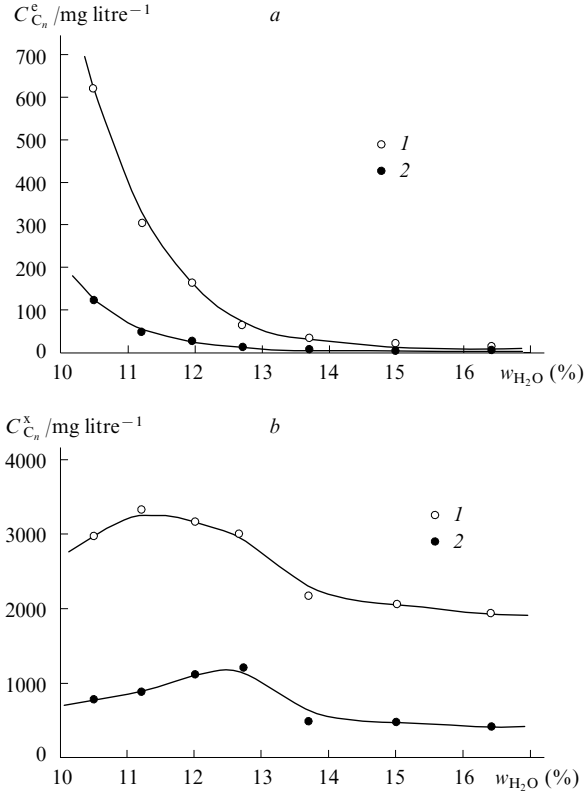


Figure 23. Concentrations of fullerenes C_{60} (*1*) and C_{70} (*2*) in the ethanol (*a*) and *o*-xylene (*b*) phases in the system $C_{60}-C_{70}-$*o*-xylene–EtOH–H_2O at 25 °C *vs.* the total content H_2O in the heterogeneous system.[73]

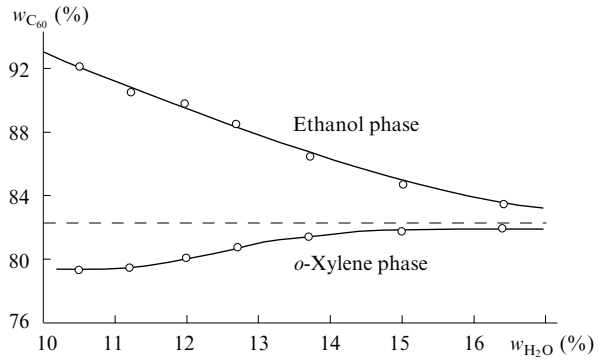


Figure 24. Relative contents of C_{60} (in the $C_{60}+C_{70}$ mixture) (mass %) in the coexisting phases *vs.* the total content of H_2O in the heterogeneous system (the dashed line shows the overall composition of the fullerene mixture distributed between the phases: 83 mass % C_{60}).[73]

Figure 24 shows the relative mass fractions of C_{60} (in the $C_{60}+C_{70}$ mixture) in the coexisting phases as a function of the total content of water (the dashed line designates the composition of the initially dissolved solid solution: 83 mass.% C_{60}). As can be seen in Fig. 24, the distribution constant (concentration ratio between *o*-xylene and ethanol) depends appreciably on the total content of H_2O; for both fullerenes, it increases with increasing water content. The relative enrichment factor $[K_{enrich}(C_{70})/K_{enrich}(C_{60})]$ monotonically increases from 1.3 (for water concentration of 10.5%) to 2.4 (for water concentration of 16.4%). Generally, it can be stated that the system $C_{60}-C_{70}-o$-xylene – ethanol – H_2O separates fullerenes C_{60} and C_{70}. Substantial advantages of this system are relatively low temperature and heat of boiling of *o*-xylene compared with 1,2,4-$Cl_3C_6H_3$ (144.4 and 213.5 °C; 43.4 and 46.1 kJ mol^{-1}); hence, the energy expenditures for evaporation and separation of the solution phases are lower.

III.7. The system $C_{60}-C_{70}$ – 1,2,4-trichlorobenzene – ethanol – H_2O

Figure 25 shows the dependence of the relative contents of C_{60} (in the $C_{60}+C_{70}$ mixture) in the coexisting phases on the C_{60} concentration in the trichlorobenzene phase at a fixed total content of water (the dashed line shows the overall composition of the fullerene mixture distributed between the phases: 72 mass % C_{60}). It can be seen from Figures 25 and 26 that the ethanol phase is always enriched in C_{60} relative to the trichlorobenzene phase. Figure 25 also indicates that the compositions of the phases approach each other following decrease in the solution concentration starting from $C^{tcb}_{C_{60}} < 700$ mg litre^{-1} (tcb is trichlorobenzene). Figure 27 shows the dependence of C_{60} and C_{70} concentrations in ethanol and trichlorobenzene on the total content of H_2O in the heterogeneous system. Figure 26 presents the dependence of the relative mass fractions of C_{60} (in the $C_{60}+C_{70}$ mixture) in the coexisting phases on the content of water. As can be seen in Figs 26 and 27, the distribution constant (concentration ratio between trichlorobenzene and ethanol phases) depends appreciably on the content of H_2O in the system. The distribution constants increase for both fullerenes with increasing water content; simultaneously, the fullerene content in the ethanol phase critically decreases. The enrichment factor also changes monotonically, being decreased from 2.2 for $w(H_2O) \approx 2.3\%$ to 1.6 for $w(H_2O) \approx 3.9\%$. It is also noteworthy that this system separates fullerenes C_{60} and C_{70}

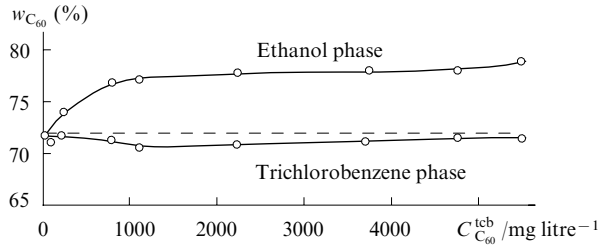


Figure 25. Relative contents of C_{60} (in the $C_{60}+C_{70}$ mixture) (mass %) in the coexisting phases *vs.* concentration of C_{60} in trichlorobenzene (C^{tcb}) in the system $C_{60}-C_{70}$ – 1,2,4-trichlorobenzene – EtOH – H_2O at 25 °C (the dashed line shows the overall composition of the fullerene mixture distributed between the phases: 72 mass % C_{60}).[75]

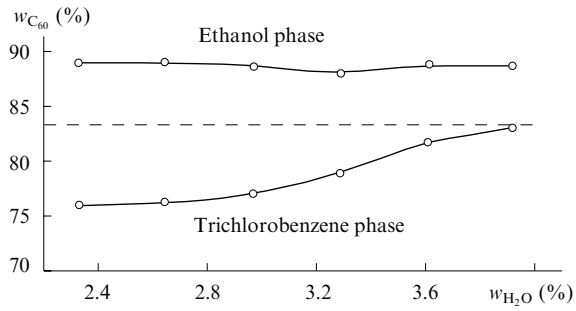


Figure 26. Relative contents of C_{60} (in the $C_{60}+C_{70}$ mixture) (mass %) in the coexisting phases *vs.* the total content of H_2O in the heterogeneous system (the dashed line shows the overall composition of the fullerene mixture distributed between the phases: 83 mass % C_{60}).[75]

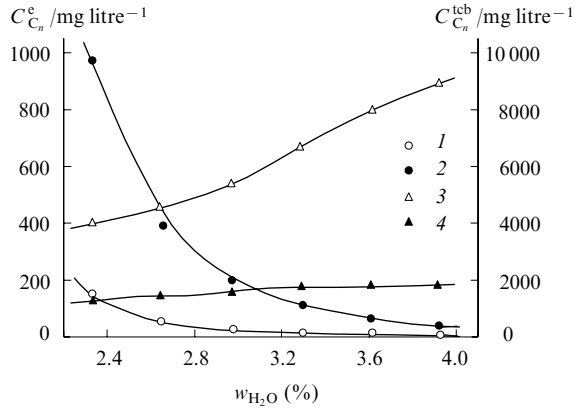


Figure 27. Concentrations of fullerenes C_{60} and C_{70} in the ethanol (C^e) and trichlorobenzene (C^{tcb}) phases in the system $C_{60}-C_{70}$ – 1,2,4-trichlorobenzene – EtOH – H_2O 25 °C *vs.* the total content of H_2O in the heterogeneous system.[75]
(*1*) C_{70} in ethanol, (*2*) C_{60} in ethanol, (*3*) C_{60} in trichlorobenzene, (*4*) C_{70} in trichlorobenzene.

much less efficiently than systems containing *o*-xylene and DMF, toluene, α-pinene and ethanol and more efficiently than the *o*-xylene and isobutylamine system, although in the present system, separation still does occur. The only important advantage of the present system is that the fullerene concentrations in both phases are high; at the minimal content of H_2O, they can be as high as >1.1 g litre^{-1} for the ethanol phase and >7.8 g litre^{-1} for the trichlorobenzene phase. This is of prime importance for development of an efficient process for commercial extractive separation of light fullerenes.

IV. Sorption equilibria in systems containing light fullerenes

The sorption properties of solids depend on a number of factors: specific surface area, specific features of the porous structure, the presence of functional groups and organic substituents on the surface and the nature of adsorbate interaction with the surface. When fullerenes are adsorbed from the liquid phase, the adsorption properties are also affected by the nature of the solvent. Evidently, all these factors are to be taken into account for selecting the optimal sorbents for fullerenes.

The theoretical aspects of interaction of fullerenes with graphite and other solids, including semiconductors (Ge, Si, GaAs) and dielectrics (LiF and MgO), have been studied by Girard *et al.*[76] The energy of dispersion interaction with the surface of these sorbents was calculated. According to Manolova *et al.*,[77] fullerene molecules are held on the carbon surface by cooperative π–π-interaction of non-planar fullerene structures, which have rings formed by sp^2-hybridized carbon atoms, with the aromatic rings present on the surface of the active carbon.

The interaction of fullerene molecules with non-planar surface areas of the carbon material should be energetically more favourable, although the accessibility of the porous structure is limited to the van der Waals volume of the fullerene molecule. Therefore, active carbons that have a great mesopore volume and the optimal specific surface area of the pores accessible for fullerene molecules are desirable for fullerene purification. It was also noted that microporous carbons are of low utility in the purification processes.

Zajac and Grozcek[78] investigated the adsorption of fullerene C_{60} from toluene solutions by the active carbons S-51 MB, S-51 WTX and DarcoG-60. The adsorption properties of active carbons towards fullerene C_{60} were compared with the properties of graphitized carbon black (Graphon). The DarcoG-60 carbon was found to possess the highest adsorption capacity and considerable irreversible adsorption; meanwhile, the adsorption of fullerene on the graphitized carbon black was fully reversible. The authors discuss the effect of the porous structure on the irreversible adsorption, in particular, overlapping of the adsorption forces from the opposite walls of narrow pores comparable in size with fullerene molecules. The irreversible adsorption is also attributable to the occurrence of polar sites detectable by butanol adsorption on the active carbon surface. However, the surface of fullerene C_{60} has no polar groups and the molecules have zero dipole moment; therefore, in our opinion, the irreversible adsorption of fullerenes on active carbons is attributable, first of all, to the presence of micropores.

A mesoporous carbon with an ordered structure synthesized using the mesoporous silica SBA-15 as the template was proposed[79] as the sorbent for fullerenes C_{60} and C_{70}. The adsorption of fullerenes on four sorbents including alumina, silica gel, active carbon and mesoporous carbon was investigated. Alumina and silica gel were shown to possess moderate adsorption capacity for fullerenes. Meanwhile, active carbon and mesoporous carbon, as expected, showed good adsorption of fullerenes, the adsorption capacity being 4 times higher for mesoporous carbon than for active carbon, which is evidently due to the specific porous structure of mesoporous carbon. Detailed measurements demonstrated that fullerene C_{70} is adsorbed on porous carbon more strongly than C_{60}. The desorption of fullerene was measured and the efficiency of using several desorption cycles was demonstrated. In particular, it was found that 47% of pure C_{60} can be desorbed in 4 cycles and ~16% of C_{70} can be desorbed in 3 cycles. The amount of desorbed C_{70} increases with temperature.

Piwonski *et al.*[80] used flow microcalorimetry to study the thermodynamics of fullerene C_{60} adsorption from toluene solutions under dynamic conditions on the surface of the mesoporous silica MCM-41. The adsorption was found to be fully reversible over the adsorbate concentration range considered, the adsorbed amount increased with increase in the fullerene concentration in the solution that flowed through the calorimetric cell. Nevertheless, even at the concentration approaching the limiting solubility of fullerene in toluene, the adsorbed amount was insufficient for the formation of a tight monolayer. Only a small portion of the total surface of silica MCM-41 was coated by fullerene molecules. After a 10 month storage and annealing, the mesoporous silica samples retained their surface area, texture and adsorption properties towards fullerene.

An improved method for fullerene purification based on filtration through a thin layer of active carbon has been reported.[81] According to the authors, this method is more convenient than column chromatography and can be used for large-scale manufacture of pure fullerenes C_{60} and C_{70}. The effects of the degree of graphitization, the presence of polar functional groups and the porous structure details on the adsorption properties of carbons was considered. The authors state that purification of fullerenes by the method they developed should be performed using carbons the pores in which are only slightly larger than fullerene molecules.

Griti and Guiochon[82] studied the adsorption of C_{60} and C_{70} over a broad concentration range on silica modified with tetraphenylporphyrin moieties; the toluene–1-methylnaphthalene system was used as the solvent. The isotherms were found to be adequately described in terms of the bi-Langmuir model. It is noteworthy that silicas with grafted aromatic groups are currently used most often in the chromatographic separation of fullerenes.

The adsorption properties of the Norit-Azo carbon towards light fullerenes have been studied.[83] The researchers used solutions of C_{60} and C_{70} in *o*-xylene, toluene and *o*-dichlorobenzene. The adsorption isotherms of fullerenes in toluene and *o*-xylene were found to be of clear-cut Langmuir nature. The static sorption capacities of the carbon (in mg of fullerenes per g of the sorbent) were: in *o*-xylene, 15.5 for C_{60} and 21.3 for C_{70}; in toluene, 14.1 for C_{60} and 14.3 for C_{70}; in *o*-dichlorobenzene, >24 for C_{60} and >25 for C_{70}. The authors state that these values are much higher

than those for most of the previously studied carbon sorbents. Hence, Norit-Azo can be considered to be an effective carbon material for the sorption purification of light fullerenes.

Multiwalled carbon nanotubes can also be promising carbon materials for the sorption and chromatography of fullerenes. They possess the set of properties required for sorbents: (1) high specific surface area; (2) inertness with respect to solvents used in the separation of fullerenes; (3) high affinity for fullerenes (this is caused by structural features, namely, the presence of six-membered carbon rings devoid of functional groups in both nanotubes and fullerenes; five-membered carbon rings are also present both in fullerenes and at the ends of nanotubes); (4) more uniform porous structure as compared with most of active carbons and the possibility to select nanotubes without micropores, which are responsible for irreversible adsorption of fullerenes; (5) relatively low cost as compared with single-walled carbon nanotubes or silica gels modified by complex organic moieties, which are widely used for chromatographic separation of fullerenes; (6) the possibility to manufacture composite sorbents with the desired service characteristics by either depositing nanotubes on hydrophobic supports or using inorganic binders.

Postnov *et al.*[84] studied the adsorption of C_{60} and C_{70} from toluene solutions on Bayer (Germany) multiwalled carbon nanotubes. The adsorption isotherms of C_{60} and C_{70} were found to have a Langmuir shape, which is also the case for carbon sorbents; the static sorption capacities of multiwalled carbon nanotubes were 22 and 18 mg g^{-1} for C_{60} and C_{70}, respectively, which is substantially higher than analogous parameters for the Norit-Azo carbon. Thus, multiwalled carbon nanotubes can be considered as efficient sorbents for light fullerenes. Also, the chromatographic properties of multiwalled carbon nanotubes and composite sorbents obtained by depositing the nanotubes on macroporous polytetrafluoroethylene were studied. The experiments were carried out in the gravity mode in toluene. The nanotubes and composite sorbents demonstrated satisfactory chromatographic properties. It was shown that the composite sorbent provides much faster chromatographic separation of C_{60} and C_{70}.

Of obvious practical interest for industrial manufacture of pure fullerenes are mineral-carbon sorbents, which combine the chemical nature of the surface of carbon materials and the porous structure of inorganic matrices. By using an inorganic support with definite porous structure and required appropriate method for deposition of the carbon layer, one can synthesize mineral-carbon sorbents with pores and specific surface areas required for the separation of fullerenes. It is possible to obtain mineral-carbon sorbents without micropores the presence of which decreases the applicability of active carbons for the separation of fullerenes. The synthesis of mineral-carbon sorbents meant for the chromatographic separation of fullerenes has been described in papers[85,86] and a patent.[87] Silochrome having uniform porous structure and large mesopores was used as the support. Carbon was chemically deposited from the gas phase under fluidized bed conditions at elevated temperature. Propargyl alcohol served as the source of carbon. The sorbents obtained in this way showed fairly high efficiency in the chromatographic separation of fullerenes in the toluene medium.

Currently, silicas modified by organic moieties with aromatic groups are used most widely for chromatographic separation of fullerenes. A drawback of these sorbents is high cost due to complexity of the synthesis and the necessity to use expensive modifying agents. Therefore, in our opinion, cheaper multiwalled carbon nanotubes and mineral-carbon sorbents could compete favourably with them in the future.

* * *

The information presented in the review on different types of phase equilibria for systems containing light fullerenes is of high practical value; this especially refers to solubility diagrams. Analysis of literature sources demonstrates that the majority of publications devoted to the solubility and extraction diagrams appeared before 2010. The reason is that the researchers' attention is currently focused on fullerene derivatives — development of methods for their synthesis, comprehensive investigation of their properties and search for applications. However, the interest in the physicochemical properties of fullerenes persists, which is directly related to the necessity to further develop the processes for isolation of light fullerenes and extend the scope of their applications. The data presented in the review can serve as the theoretical basis for the development of industrial processes for manufacture, separation and purification of light fullerenes and for the synthesis of nanomaterials based on them.

This review was supported by the Russian Foundation for Basic Research (Project No. 15-08-08438K), grants of RF President MC-4657.2015.3 and MD-4650.2015.3 and grant of the Saint Petersburg State University for the support of scientific research carried out under supervision of prominent scientists 'creation and *in vitro* study of interactions of receptor – ligand pairs needed for the development of new strategies for the therapy of socially significant diseases and elaboration of methods for biological functionalization of the surface of materials for medical purposes (living and artificial implants).' The solubility of fullerenes was studied at the resource centre Geomodel of the SPbSU.

References

1. K N Semenov, N A Charykov, V A Keskinov, A K Piartman, A A Blokhin, A A Kopyrin *J. Chem. Eng. Data* **55** 13 (2010)
2. N O Mchedlov-Petrossyan *Chem. Rev.* **113** 5149 (2013)
3. R S Ruoff, D S Tse, R Malhotra, D C Lorents *J. Phys. Chem.* **97** 3379 (1993)
4. N Sivaraman, R Dhamodaran, I Kalliappan, T G Srinivasan, P R Vasudeva Rao, C K Mathews *J. Org. Chem.* **57** 6077 (1992)
5. V N Bezmel'nitsyn, A V Eletskii, M V Okun' *Usp. Fiz. Nauk* **168** 1091 (1998) [*Usp. Fiz. Nauk* **168** 1195 (1998)]
6. K N Semenov, N A Charykov, O V Arapov *Russ. J. Phys. Chem. A* **82** 1318 (2008) [*Zh. Fiz. Khim.* **82** 1483 (2008)]
7. K N Semenov, N A Charykov, A K Pyartman, V A Keskinov, O V Arapov, N I Alekseev, V V Lishchuk *Russ. J. Phys. Chem. A* **82** 728 (2008) [*Zh. Fiz. Khim.* **82** 843 (2008)]
8. K N Semenov, N A Charykov, O V Arapov, V A Keskinov, A K Pyartman, M S Gutenev, O V Proskurina, M Yu Matuzenko, V V Klepikov *Russ. J. Phys. Chem. A* **82** 1045 (2008) [*Zh. Fiz. Khim.* **82** 1183 (2008)]

9. K N Semenov, N A Charykov, A K Pyartman,V A Keskinov, O V Arapov, N I Alekseev, V V Lishchuk *Russ. J. Appl. Chem.* **80** 557 (2007) [*Zh. Prikl. Khim.* **80** 570 (2007)]
10. M I Shakhparonov *Vvedenie v Molekulyarnuyu Teoriyu Rastvorov* (Introduction to a Molecular Theory of Solutions) (Moscow: Gos. Izd. Tekhniko-Teoret. Lit., 1956)
11. X Zhou, J Liu, Z Jin, Z Gu, Y Wu, Y Sun *Fullerene Sci. Technol.* **5** 285 (1997)
12. W A Scrivens, J M Tour *J. Chem. Soc., Chem. Commun.* 1207 (1993)
13. K Semenov, N Charykov *Rastvorimost' Legkikh Fullerenov i ikh Proizvodnykh* (Solubility of Light Fullerenes and Their Derivatives) (Saarbrücken, Germany: LAP LAMBERT Academic Publ., 2011)
14. E B Stukalin, N V Avramenko, M V Korobov, R Ruoff *Fullerene Sci. Technol.* **9** 113 (2001)
15. F Michaud, M Barrio, D O López, J Ll Tamarit, V Agafonov, S Toscani, H Szwarc, R Céolin *Chem. Mater.* **12** 3595 (2000)
16. D Heymann *Lunar Planet. Sci.* **27** 543 (1996)
17. L B Piotrovskii, O I Kiselev *Fullereny v Biologii* (Fullerenes in Biology) (St Petersburg: Rostok, 2006)
18. N Arsalani, K E Geckeler *Fullerene Sci. Technol.* **4** 897 (1996)
19. A N Kirgintsev, L N Trushnikova, V G Lavrent'eva *Rastvorimost' Neorganicheskikh Veshchestv v Vode* (Solubility of Inorganic Substances in Water) (Leningrad: Khimiya, 1972)
20. R Céolin, D O López, M Barrio, J Ll Tamarit, P Espeau, B Nicolaï, H Allouchi, R Papoular *Chem. Phys. Lett.* **399** 401 (2004)
21. M-F Gardette, A Chilouet, S Toscani, H Allouchi, V Agafonov, J-C Rouland, H Szwarc, R Céolin *Chem. Phys. Lett.* **306** 149 (1999)
22. A L Smith, E Walter, M V Korobov, O L Gurvich *J. Phys. Chem.* **100** 6775 (1996)
23. M V Korobov, A L Mirak'yan, N V Avramenko, R Ruoff *Dokl. Akad. Nauk* **349** 346 (1996)
24. N V Avramenko, E B Stukalin, M V Korobov, I S Neretin, Yu L Slovokhotov *Thermochim. Acta* **370** 21 (2001)
25. M V Korobov, A L Mirakian, N V Avramenko, E F Valeev, I S Neretin, Yu L Slovokhotov, A L Smith, G Olofsson, R S Ruoff *J. Phys. Chem. B* **102** 3712 (1998)
26. V N Bezmel'nitsyn, A V Eletskii, E V Stepanov *Zh. Fiz. Khim.* **69** 735 (1995)
27. M Korobov, A Smith, in *Fullerenes: Chemistry, Physics, and Technology* (Eds K M Kadish, R S Ruoff) (New York: Wiley, 2000) p. 53
28. K N Semenov, N A Charykov, O V Arapov *Fullerene Sci. Technol.* **17** 230 (2009)
29. P Ruelle, A Farina-Cuendet, U W Kesselring *J. Am. Chem. Soc.* **118** 1777 (1996)
30. I Prigogine, R Defay *Chemical Thermodynamics* (New York: Wiley, 1954)
31. D Heymann *Carbon* **34** 627 (1996)
32. K N Semenov, N A Charykov, O V Arapov *Vestn. SPbGU, Ser. 4* (1) 70 (2008)
33. M H Herbst, G H M Dias, J G Magalhães, R B Tôrres, P L O Volpe *J. Mol. Liq.* **118** 9 (2005)
34. L N Sidorov, M A Yurovskaya, A Ya Borshchevskii, I V Trushkov, I N Ioffe *Fullereny* (Fullerenes) (Moscow: Ekzamen, 2005)
35. K N Semenov, N A Charykov, V N Postnov, O A Krokhina, E G Gruzinskaya *Russ. J. Gen. Chem.* **80** 2443 (2010) [*Zh. Obshch. Khim.* **80** 1981 (2010)]
36. C M Hansen *Hansen Solubility Parameters: A User's Handbook* (Boca Raton, FL: CRC Press, 2007)
37. Y Marcus, A L Smith, M V Korobov, A L Mirakyan, N V Avramenko, E B Stukalin *J. Phys. Chem. B* **105** 2499 (2001)
38. C M Hansen, A L Smith *Carbon* **42** 1591 (2004)
39. S M Danauskas, P C Jurs *J. Chem. Inf. Comput. Sci.* **41** 419 (2001)
40. I Z Kiss, G Mándi, M T Beck *J. Phys. Chem. A* **104** 8081 (2000)
41. F Gharagheizi, R F Alamdari *Fullerenes, Nanotubes, Carbon Nanostruct.* **16** 40 (2008)
42. S Sawamura, F Nobuyuki *Chem. Phys. Lett.* **299** 177 (1999)
43. S Sawamura, N Fujita *Carbon* **45** 965 (2007)
44. I I Adamenko, L A Bulavin, K O Moroz, Yu I Prylutskyy, P Scharff *J. Mol. Liq.* **105** 149 (2003)
45. A N Ponomarev, B M Aksel'rod, V T Barchenko, V P Belousov, Z S Egorova, I V Igonchenkov, A Yu Isakov, O Yu Kut'eva, V A Nikitin, D V Nikitin, S V Ruzaev, A V Rumyantsev, O S Tulyakov, N A Charykov, M E Yudovich, A L Yurin *Russ. J. Phys. Chem. A* **74** 1942 (2000) [*Zh. Fiz. Khim.* **74** 2134 (2000)]
46. K N Semenov, N A Charykov, O V Arapov, N I Alekseev, M A Trofimova *Russ. J. Phys. Chem. A* **83** 59 (2009) [*Zh. Fiz. Khim.* **83** 72 (2009)]
47. K N Semenov, N A Charykov, N I Alekseyev, O V Arapov *J. Chem. Eng. Data* **54** 756 (2009)
48. O V Arapov, B M Aksel'rod, A A Pronkin, N A Charykov, O Yu Ryazanova *Russ. J. Appl. Chem.* **76** 33 (2003) [*Zh. Prikl. Khim.* **76** 39 (2003)]
49. A M Kolker, N I Islamova, N V Avramenko, A V Kozlov *Russ. J. Phys. Chem. A* **80** 1622 (2006) [*Zh. Fiz. Khim.* **80** 1825 (2006)]
50. A M Kolker, N I Islamova, N V Avramenko, A V Kozlov *J. Mol. Liq.* **131 – 132** 95 (2007)
51. A M Kolker, A V Kozlov *Russ. J. Phys. Chem. A* **86** 715 (2012) [*Zh. Fiz. Khim.* **86** 805 (2012)]
52. A M Kolker, A V Kozlov, M S Gruzdev, V A Sharnin *Fullerenes, Nanotubes, Carbon Nanostruct.* **19** 435 (2011)
53. M T Beck *Pure Appl. Chem.* **70** 1881 (1998)
54. M T Beck, G Mándi *Fullerene Sci. Technol.* **5** 291 (1997)
55. P P Kulkarni, C T Jafvert *Environ. Sci. Technol.* **42** 845 (2008)
56. C T Jafvert, P P Kulkarni *Environ. Sci. Technol.* **42** 5945 (2008)
57. J M Prausnitz, R N Lichtenthaler, E Gomes de Azevedo *Molecular Thermodynamics of Fluid-Phase Equilibria* (Englewood Cliffs, NJ: Prentice-Hall, 1986)
58. T Braun, L Márk, R P Ohmacht, U Sharma *Fullerenes, Nanotubes, Carbon Nanostruct.* **15** 311 (2007)
59. Patent RF 2198136 (2001)
60. Patent RF 2214226 (2003)
61. Patent RF 2284293 (2006)
62. Patent RF 2283273 (2006)
63. K N Semenov, N A Charykov, V I Namazbaev, O V Arapov, V V Pavlovetz, V A Keskinov, A K Pyartman *Russ. J. Gen. Chem.* **79** 1683 (2009) [*Zh. Obshch. Khim.* **79** 1323 (2009)]
64. F Cataldo, T Braun *Fullerenes, Nanotubes, Carbon Nanostruct.* **15** 331 (2007)
65. *Medicinal Chemistry and Pharmacological Potential of Fullerenes and Carbon Nanotubes* (Eds F Cataldo, T Da Ros) (Springer, 2008)
66. K N Semenov, D G Letenko, N A Charykov, V A Nikitin, M Yu Matuzenko, V A Keskinov, V N Postnov, A A Kopyrin *Russ. J. Appl. Chem.* **84** 44 (2011) [*Zh. Prikl. Khim.* **84** 44 (2011)]
67. K N Semenov, N A Charykov, V I Namazbaev, O V Arapov, V V Pavlovets, V A Keskinov, A K Pyartman, E N Strogonova, N M Saf'yannikov *Vestn. SPbGU, Ser. 4* (3) 80 (2009)
68. V V Golubkov, B A Shakhmatkin, N A Charykov, B M Aksel'rod *Russ. J. Phys. Chem. A* **76** 482 (2002) [*Zh. Fiz. Khim.* **76** 562 (2002)]

69. K N Semenov, N A Charykov, O V Arapov, E N Strogonova, N M Saf'yannikov *Vestn. SPbGU. Ser. 4* (1) 140 (2009)
70. S Talukdar, P Pradhan, A Banerji *Fullerene Sci. Technol.* **5** 547 (1997)
71. O V Arapov, N A Charykov, V I Seregin, K V Nekrasov, V I Gerasimov, K B Strel'nikov, A A Pronkin, V V Klepikov *Tech. Phys. Lett.* **29** 119 (2003) [*Pis'ma Zh. Tekh. Fiz.* **29** (3) 74 (2003)]
72. O V Arapov, A A Pronkin, N A Charykov, V I Seregin, K B Strel'nikov *Russ. J. Appl. Chem.,* **76** 37 (2003) [*Zh. Prikl. Khim.* **76** 35 (2003)]
73. V A Keskinov, A K Pyartman, S V Pundelik, O V Arapov, V I Seregin, K B Strel'nikov, O S Alekhin, V I Gerasimov, K V Nekrasov, in *XIII Verossiiskaya Konferentsiya po Ekstraktsii (Tez. Dokl.)* [The XIIIrd All-Russian Conference on Extraction (Abstracts of Reports), Moscow, 2004] Pt. 1, p. 83
74. O V Arapov, N D Abovskii, N A Charykov, V I Seregin, K V Nekrasov, V I Gerasimov *Russ. J. Appl. Chem.,* **79** 166 (2006) [*Zh. Prikl. Khim.* **79** 167 (2006)]
75. O V Arapov, K N Semenov, N A Charykov, V I Seregin, K V Nekrasov, V I Gerasimov *Russ. J. Appl. Chem.,* **79** 201 (2006) [*Zh. Prikl. Khim.* **79** 203 (2006)]
76. C Girard, P Lambin, A Dereux, A A Lucas *Phys. Rev. B* **49** 11425 (1994)
77. N Manolova, I Rashkov, D Legras, S Delpeux, F Beguin *Carbon* **33** 209 (1995)
78. J Zajac, A J Groszek *Carbon* **35** 1053 (1997)
79. H Wang, F L Y Lam, X Hu, K M Ng *Langmuir* **22** 4583 (2006)
80. I Piwonski, J Zajac, D J Jones, J Rozière, S Partyka, S Plaza *Langmuir* **16** 9488 (2000)
81. N Komatsu, T Ohe, K Matsushige *Carbon* **42** 163 (2004)
82. F Gritti, G Guiochon *J. Chromatogr., A* **1053** 59 (2004)
83. K N Semenov, V I Seregin, O V Arapov, N A Charykov *Russ. J. Appl. Chem.* **77** 1627 (2004) [*Zh. Prikl. Khim.* **77** 1638 (2004)]
84. V N Postnov, A Ya Scaletskaya, O A Krokhina, V A Keskinov, N A Charykov, K N Semenov *Nanosystems: Phys., Chem., Math.* **4** 706 (2013)
85. O A Krokhina, V N Postnov *Nanotekhnika* (2) 39 (2010)
86. V N Postnov, O A Krokhina *Nanotekhnika* (1) 78 (2013)
87. Patent RF 2373992 (2008)